UNIVERSITY OF CALIFORNIA
SANTA CRUZ

UNLOCKING THE THERAPEUTIC POTENTIAL OF AGOUTI SIGNALING PEPTIDE

A thesis submitted in partial satisfaction
of the requirements for the degree of

MASTER OF SCIENCE

in

CHEMISTRY

by

Jillian L. Miller

March 2017

The Thesis of Jillian L. Miller is approved:

_____
Professor Seth M. Rubin, Chair

_____
Professor Glenn L. Millhauser

_____
Professor Carrie L. Partch

_____
Tyrus Miller
Vice Provost and Dean of Graduate Studies

TABLE OF CONTENTS

TABLE OF FIGURES

ABSTRACT

Unlocking the Therapeutic Potential of Agouti Signaling Peptide

Jillian L. Miller

Agouti Signaling Peptide (ASIP) is a small disulfide-rich peptide, which acts as an inverse agonist at melanocortin receptor 1 (MC1R) and reduces the production of melanin. ASIP has recently been shown to increase melanoma treatment sensitivity. Here we develop strategies to improve ASIP potency by increasing its affinity and specificity to MC1R. We find no increase in binding for the constructs we synthesized. We then increase the stability of ASIP via head-to-tail cyclization using hydrazide intermediates to facilitate native chemical ligation. We find the imposed chemical restraint does not alter peptide structure or function as a melanocortin antagonist. We compared the stability of linear and cyclic ASIP in human serum, finding that cyclic ASIP has a slight increase in resistance to proteolysis. These studies have the potential to revolutionize the treatment of melanoma through the use of ASIP as a peptide therapeutic.

ACKNOWLEDGEMENTS

This work could never have been completed without the support of my advisers, peers, and family members. I would especially like to thank Professor Glenn Millhauser, Professor Set Rubin, Professor Carrie Partch, and Professor Bill Scott. I am grateful for the support and training from numerous graduate student peers and mentors within the Millhauser group: Matt Nix, Ann Spevacek, Chris Dudzik, Eric Evans, Alex McDonald, Mike Madonna, Rafael Palomino, Valerie Chen, Kate Markham, Graham Roseman, and Kevin Schilling. I mentored many undergraduate students, sometimes three students at a time. I want to thank Eveline Junaedy, Cynthia Lai, Shannon Lee, Rodrigo Andrade, Alfonso Zavala-Chavez, Andrew Martinez, and Beau Norgeot. Also, thank you to Beau Norgeot for being a friend as well as an undergraduate researcher. Many people at UCSC helped and supported me. Although I can't list you all, thank you. A special thank you to Rebecca Roha for all your support, scientific and otherwise. Lastly, I am thankful for my parents and younger siblings.

The text of this thesis includes excerpts from the text and figures of an unpublished manuscript: Backbone Cyclization of Agouti-Family Knottins. The Co-author Professor Glenn Millhauser listed in this publication directed and supervised the research that forms the basis of this thesis.

CHAPTER 1
INTRODUCTION

The Melanocortin System

Melanocortin receptors are expressed throughout the body and control diverse physiological functions, including pigmentation and energy balance (1,2). G-protein-coupled receptors (GPCRs) comprise over 1000 different types of receptors and include the melanocortin receptors (3). Traditionally, a GPCR will be activated by one or more agonists and be inactive in the absence of agonist. The melanocortin system diverges from this classical model because it contains endogenous antagonists as well as agonists (4). This complexity can give insight into the behavior of receptor-ligand systems.

The endogenous agonists in the melanocortin system are derived from proopiomelanocortin (POMC) (5). This proprotein is expressed in many different tissues throughout the body including the skin, the lymphoid system, and the hypothalamus (6). The proteolysis of POMC is tissue specific and can result in four different products: adrenocorticotropic hormone (ACTH), α-melanocyte stimulating hormone (α-MSH), β-MSH, or γ-MSH (7). These agonists are short, unstructured peptides between 11 and 39 residues in length and have a conserved His-Phe-Arg-Trp motif (2,8).

Agouti signaling peptide (ASIP) and agouti-related peptide (AgRP) are unique in that they are the first endogenous antagonists in a GPCR system (4). They compete with the agonists at the same binding pocket, using slightly different binding sequences (2,9). They also decrease constitutive activity of the receptor, making them inverse

agonists (4). The β-defensins, previously known to have innate immune properties, are recent additions to this system (10). They bind to the melanocortin receptors with high affinity and act as neutral antagonists (10–12).

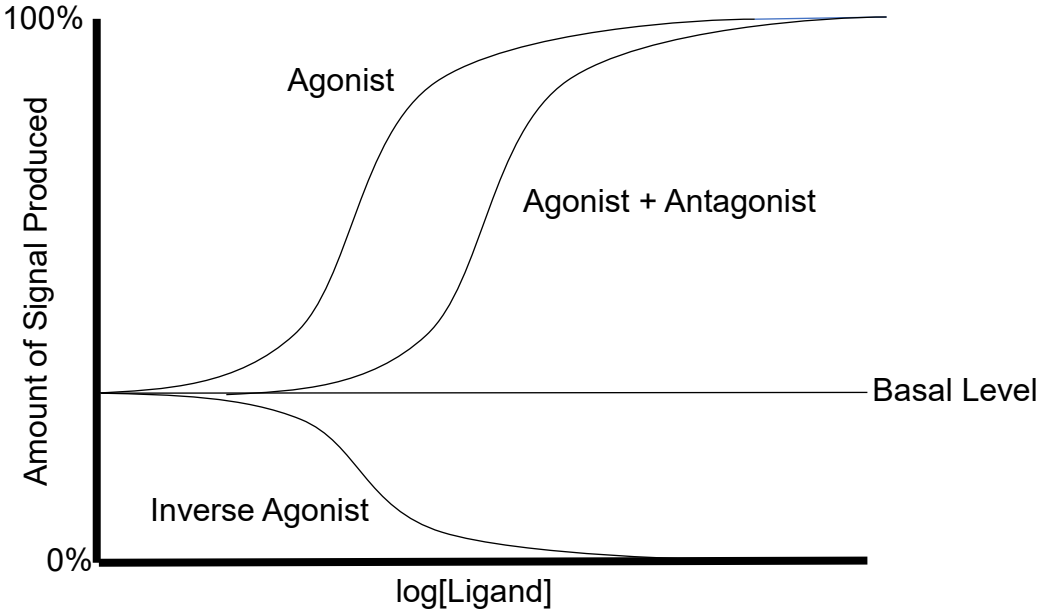

Figure 1.1. Agonists, Antagonists, and Inverse Agonists
The agonist curve is sigmoidal, showing an increase of signal as the agonist concentration increases, until the receptor is saturated. Antagonist shifts this curve to the right. As the antagonist competes for the binding pocket, more agonist is needed to achieve the same amount of signal. Inverse agonist reduces the signal below basal levels.

Melanocortin Receptor Structures

All melanocortin receptors have 7 transmembrane helices and are imbedded in the cell membrane (13,14). It is notoriously difficult to solve the structures of membrane proteins. Until 2007, the only eukaryotic GPCR to have a crystal structure was rhodopsin, the photoreceptor responsible for vision. The *in vitro* structures for melanocortin receptors are not known, but there are *in silico* models based on rhodopsin (15).

These receptors are functionally coupled to adenylate cyclase, activating a cAMP-dependent signaling pathway (2). The receptors transmit signals across this membrane and amplify them in the process. Due to the amplification of downstream effects, along with the prevalence of these receptors in most biological processes, GPCRs are a common drug target (16).

Melanocortin receptors are known for their high constitutive activity. Much of the basal activity of melanocortin receptor 4 (MC4R) is due to self-activation. The extracellular N-terminus of the receptor interacts with its binding pocket, acting as its own agonist (17). It is feasible that this occurs with MC1R as well.

Ligand Structures

α-MSH is a 13-amino acid peptide with an acetylated N-terminus and an amidated C-terminus (2). The sequence is Ac-SYSMEHFRWGKPV-NH_2. A more potent, synthetic version of this peptide has two modifications: a norleucine in position 4 and a D-phenylalanine in position 7 (2,18).

In vivo, ASIP and AgRP are 132 amino acids and 50 amino acids respectively and both peptides contain 5 disulfide bridges in their structured C-terminus (19,20). Two core disulfides, with a third disulfide threading though their loop, form an inhibitor cystine knot (ICK) motif, previously found only in plants and invertebrate toxins. This fold lends a significant amount of stability to the peptide. However, further stability is possible by end-to-end cyclization (see Chapter 3).

ASIP-YY is a more manageable form of this difficult peptide. It includes only the last 53 amino acids of the native sequence. Previous work in this lab determined that solubility is improved by including the naturally-occurring 13 amino acids prior to the first cysteine (19). This extends into the arginine/lysine rich region from positions 57 to 86. In addition, oxidative folding is greatly improved by the point mutations Q115Y and S124Y. These point mutations and the truncation centered on the structured Cys-rich region are based on AgRP's sequence, because AgRP folds well *in vitro* and its structured domain is sufficient for binding (19).

A MDVTRLLLATLLVFLCFFTANSHLPPEEKLRDDRSLRSNSSVNLLDVPSVSIVALNK
KSKQIGRKAAEKKRSSKKEASMKKVVRPRTPLSAPCVATRNSCKPPAPACCDPCASC
QCRFFRSACSCRVLSLNC

B KKVVRPRTPLSAPCVATRNSCKPPAPACCDPCASCYCRFFRSACYCRVLSLNC

Figure 1.2. Wild Type ASIP and ASIP-YY
(A) The full ASIP sequence including the signal peptide (orange), lysine/arginine rich region (blue), and cysteine rich region (green). The underlined portions indicate the 13 amino acids before the first cysteine added to ASIP-YY and the location of the two point mutations. (B) The final ASIP-YY sequence, including the 13 amino acids added for solubility (purple) and the two tyrosine mutations (red).

The smaller β-defensins only have 3 disulfides and as part of the innate immune system, they use their positive surface potential to damage the membranes of bacteria and other pathogens (10,21,22). *In vitro*, β-defensins and ASIP are often difficult to oxidatively fold because of the many possible disulfide connectivities (12,19). β-defensins have 15 possible connectivities and ASIP has 945 choices.

Receptor Binding

The disulfides in ASIP and AgRP break the structures into 3 main loops. The active loop fits deeply into the binding pocket of the melanocortin receptor (15). It contains the binding motif Arg-Phe-Phe, discovered using alanine scanning, and is necessary for high affinity melanocortin receptor binding (9). The N-terminal loop is necessary for robust binding to MC4R (23). Recent work done by Patel et al. shows that ASIP's C-terminal loop is necessary for inverse agonism at MC1R (24). While AgRP does not bind to MC1R, many sequence mutations and truncations do not alter its tight binding to MC4R (23,25). These results suggest that small mutations to ASIP will also continue to bind to melanocortin receptors with high affinity (see Chapter 2 where this was disproved).

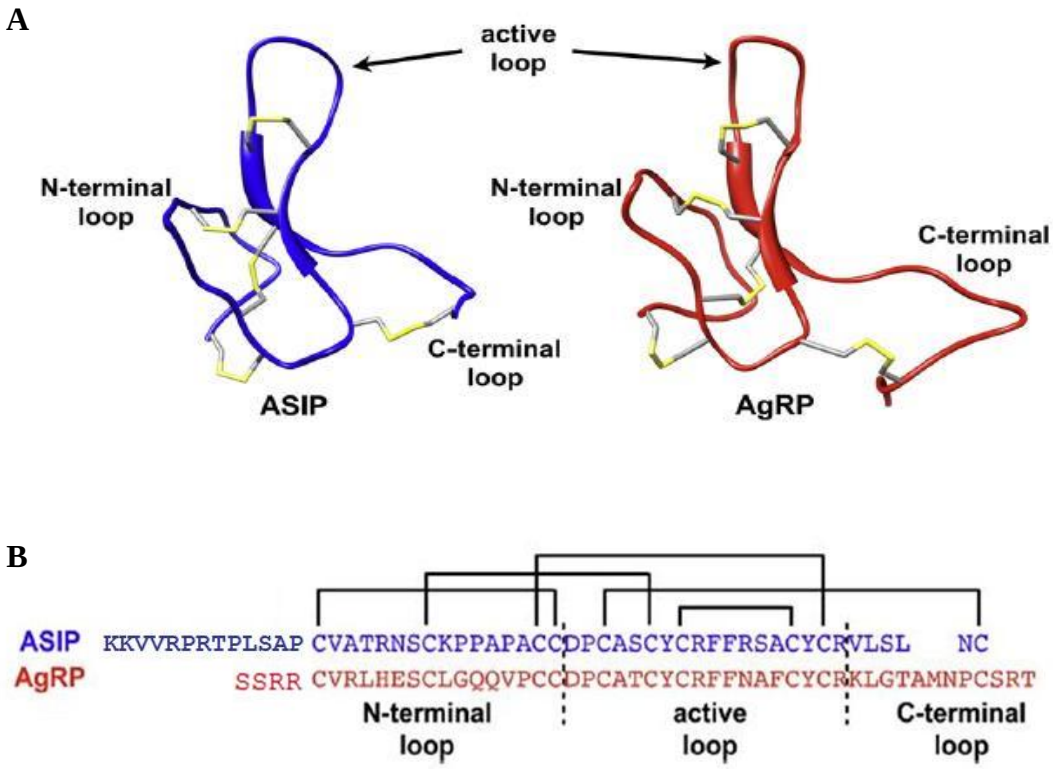

Figure 1.3. Structures of ASIP and AgRP
(A) ASIP (blue) and AgRP (red) with the active loops, N-terminal loops, and C-terminal loops labeled. Each peptide has 5 disulfide bridges (yellow stick representations). Reproduced from Patel et al (24). (B) A comparison of the ASIP-YY sequence (blue) to the AgRP sequence (red). The loop separations (dotted lines) are determined by the shared cysteine placement and connectivity (black brackets). Adapted from Patel et al (24).

In contrast, β-defensins bind to melanocortin receptors using patches of positive charge. Nix et al. attempted to find a specific amino acid sequence responsible for binding but only mutating large patches of the peptide fully reduced binding (11). They concluded that binding was solely based on electrostatics. The melanocortin receptors' binding pockets have a very negative electrostatic potential that complements the critically placed positive charges on the β-defensins (11).

Melanocortin Receptor 1 and Melanogenesis

MC1R is primarily expressed in the epidermis and controls eumelanin production. Eumelanin is a dark black or brown pigment that prevents UV damage to DNA. Eumelanin is produced in melanocytes and transported to surrounding skin cells in organelles called melanosomes (26).

α-MSH acts as an agonist at the receptor, leading to an increase in the secondary messenger cAMP and a downstream increase in eumelanin production (3). ASIP acts as an inverse agonist and decreases basal cAMP levels. Treatment with ASIP will lead to a decrease in eumelanin, leading to a phenotype dominated by pheomelanin, a red or yellow pigment. This has been extensively studied in mice. Controlled expression of ASIP in wild type mice will lead to a brown/yellow/brown banding pattern. Overexpression of ASIP prevents α-MSH from binding and leads to a yellow phenotype (27).

Ubiquitous expression of ASIP in rodents will not only lead to a yellow/red phenotype, but will also lead to obesity (28). This is due to ASIP binding to MC4R in the brain, leading to an increased appetite and increased energy storage. This phenotype led to the discovery of the ASIP homolog expressed in the brain, AgRP (28).

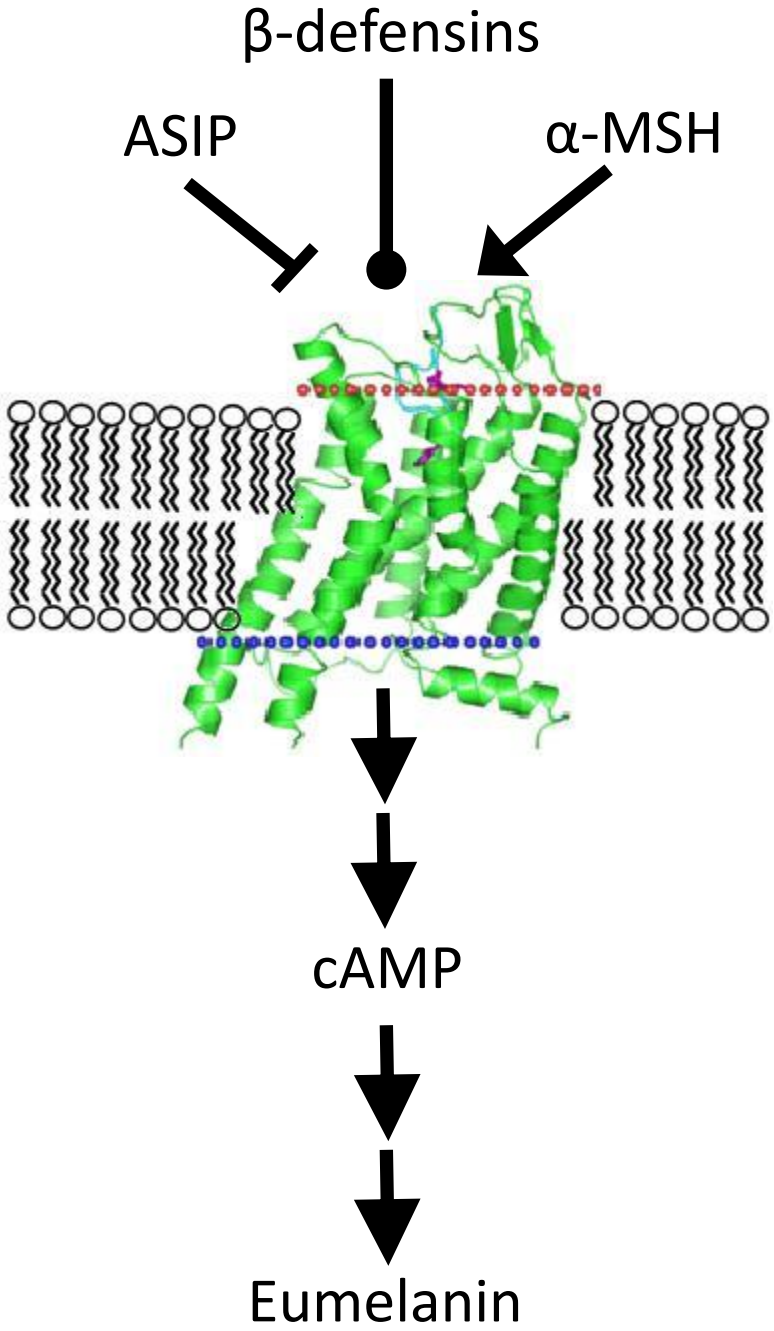

Figure 1.4. MC1R Model and Ligands
ASIP is an inverse agonist, β-defensins are neutral antagonists, and α-MSH is an agonist at MC1R (green). Activation of this receptor leads to an increase of the secondary messenger cAMP and a downstream production of eumelanin. The receptor model and positioning within the membrane are reproduced from Pogozheva et al (29,30).

Melanoma

American Cancer Society estimates that 76,380 new melanomas will be diagnosed in the US in 2016 (31). Over 10,000 Americans will die of melanoma this year. Melanoma is more likely than other skin cancers to metastasize and it causes the majority of skin cancer deaths (31). It is very resistant to chemotherapy because melanosomes sequester and even transfer chemotherapeutics outside of the cell (32,33). Consequently, the chemotherapeutic agent cannot effectively reach the nucleus, an essential step for crosslinking the DNA and initiating the apoptosis pathway (32,33). In collaboration with Maria Wei's group at UCSF, we demonstrated we could use ASIP to reduce the number of mature melanosomes. We also found that ASIP sensitizes melanoma cells to chemotherapy, making it two to three times as effective (32).

The Therapeutic Potential of ASIP

There are many benefits to using peptides are therapeutics. Compared to small molecules, the complexity of amino acid sequences can lead to higher target specificity and tighter binding (34,35). ASIP, being a normal protein found in skin, is non-toxic and is anticipated to have minimal side effects.

However, there are also some problems as well. Most biologics must be injected intravenously rather than ingested orally and absorbed through the digestive track (36,37). In addition, peptides are also highly susceptible to proteases. This process can be slowed via cyclization. End-to-end cyclization eliminates the termini of

peptides, preventing exoproteases from acting. It also quiets internal motion and prevents endoproteases from degrading the peptide. Cyclization reduces conformational freedom that could lead to binding promiscuity and thereby could increase specificity for the target receptor. In some cases, it increases drug potency or limits protein unfolding at high temperatures (36,37).

Thesis Outline

The overall goal of this work is to biophysically characterize several modified ASIP constructs and their interactions at MC1R. Chapter 2 proposes ASIP's potential as a therapeutic and describes several ASIP mutations designed to increase the binding affinity and specificity for MC1R. Chapter 3 will examine the benefits of cyclizing ASIP, along with a detailed protocol for end-to-end cyclization.

References

1. Gantz I, Fong TM. The melanocortin system. Am J Physiol Endocrinol Metab. 2003 Mar;284(3):E468-474.

2. Abdel-Malek ZA. Melanocortin receptors: their functions and regulation by physiological agonists and antagonists. Cell Mol Life Sci CMLS. 2001 Mar;58(3):434–41.

3. Wikberg JE, Muceniece R, Mandrika I, Prusis P, Lindblom J, Post C, et al. New aspects on the melanocortins and their receptors. Pharmacol Res. 2000 Nov;42(5):393–420.

4. Milligan G. Constitutive activity and inverse agonists of G protein-coupled receptors: a current perspective. Mol Pharmacol. 2003 Dec;64(6):1271–6.

5. Wikberg JE. Melanocortin receptors: perspectives for novel drugs. Eur J Pharmacol. 1999 Jun 30;375(1–3):295–310.

6. Hadley ME, Haskell-Luevano C. The proopiomelanocortin system. Ann N Y Acad Sci. 1999 Oct 20;885:1–21.

7. Wintzen M, Gilchrest BA. Proopiomelanocortin, its derived peptides, and the skin. J Invest Dermatol. 1996 Jan;106(1):3–10.

8. Bednarek MA, Silva MV, Arison B, MacNeil T, Kalyani RN, Huang RR, et al. Structure-function studies on the cyclic peptide MT-II, lactam derivative of alpha-melanotropin. Peptides. 1999;20(3):401–9.

9. Kiefer LL, Veal JM, Mountjoy KG, Wilkison WO. Melanocortin receptor binding determinants in the agouti protein. Biochemistry (Mosc). 1998 Jan 27;37(4):991–7.

10. Candille SI, Kaelin CB, Cattanach BM, Yu B, Thompson DA, Nix MA, et al. A B-defensin mutation causes black coat color in domestic dogs. Science. 2007 Nov 30;318(5855):1418–23.

11. Nix MA, Kaelin CB, Ta T, Weis A, Morton GJ, Barsh GS, et al. Molecular and Functional Analysis of Human β-Defensin 3 Action at Melanocortin Receptors. Chem Biol. 2013 Jun;20(6):784–95.

12. Nix MA, Kaelin CB, Palomino R, Miller JL, Barsh GS, Millhauser GL. Electrostatic Similarity Analysis of Human β-Defensin Binding in the Melanocortin System. Biophys J. 2015 Nov;109(9):1946–58.

13. Hanson MA, Stevens RC. Discovery of new GPCR biology: one receptor structure at a time. Struct Lond Engl 1993. 2009 Jan 14;17(1):8–14.

14. Gilman AG. G proteins: transducers of receptor-generated signals. Annu Rev Biochem. 1987;56:615–49.

15. Chai B-X, Pogozheva ID, Lai Y-M, Li J-Y, Neubig RR, Mosberg HI, et al. Receptor−Antagonist Interactions in the Complexes of Agouti and Agouti-Related Protein with Human Melanocortin 1 and 4 Receptors † , ‡. Biochemistry (Mosc). 2005 Mar;44(9):3418–31.

16. Fredriksson R, Lagerström MC, Lundin L-G, Schiöth HB. The G-protein-coupled receptors in the human genome form five main families. Phylogenetic analysis, paralogon groups, and fingerprints. Mol Pharmacol. 2003 Jun;63(6):1256–72.

17. Ersoy BA, Pardo L, Zhang S, Thompson DA, Millhauser G, Govaerts C, et al. Mechanism of N-terminal modulation of activity at the melanocortin-4 receptor GPCR. Nat Chem Biol. 2012 Jun 24;8(8):725–30.

18. Mountjoy KG. The human melanocyte stimulating hormone receptor has evolved to become “super-sensitive” to melanocortin peptides. Mol Cell Endocrinol. 1994 Jun;102(1–2):R7-11.

19. McNulty JC, Jackson PJ, Thompson DA, Chai B, Gantz I, Barsh GS, et al. Structures of the agouti signaling protein. J Mol Biol. 2005 Mar 4;346(4):1059–70.

20. McNulty JC, Thompson DA, Bolin KA, Wilken J, Barsh GS, Millhauser GL. High-resolution NMR structure of the chemically-synthesized melanocortin receptor binding domain AGRP(87-132) of the agouti-related protein. Biochemistry (Mosc). 2001 Dec 25;40(51):15520–7.

21. Pazgier M, Hoover DM, Yang D, Lu W, Lubkowski J. Human β-defensins. Cell Mol Life Sci CMLS. 2006 Jun 1;63(11):1294–313.

22. Yang D, Chertov O, Bykovskaia SN, Chen Q, Buffo MJ, Shogan J, et al. Beta-defensins: linking innate and adaptive immunity through dendritic and T cell CCR6. Science. 1999 Oct 15;286(5439):525–8.

23. Jackson PJ, McNulty JC, Yang Y-K, Thompson DA, Chai B, Gantz I, et al. Design, pharmacology, and NMR structure of a minimized cystine knot with agouti-related protein activity. Biochemistry (Mosc). 2002 Jun 18;41(24):7565–72.

24. Patel MP, Cribb Fabersunne CS, Yang Y, Kaelin CB, Barsh GS, Millhauser GL. Loop-Swapped Chimeras of the Agouti-Related Protein and the Agouti Signaling

Protein Identify Contacts Required for Melanocortin 1 Receptor Selectivity and Antagonism. J Mol Biol. 2010 Nov;404(1):45–55.

25. Madonna ME, Schurdak J, Yang Y-K, Benoit S, Millhauser GL. Agouti-related protein segments outside of the receptor binding core are required for enhanced short- and long-term feeding stimulation. ACS Chem Biol. 2012 Feb 17;7(2):395–402.

26. Abdel-Malek ZA, Knittel J, Kadekaro AL, Swope VB, Starner R. The melanocortin 1 receptor and the UV response of human melanocytes--a shift in paradigm. Photochem Photobiol. 2008 Apr;84(2):501–8.

27. Barsh G, Gunn T, He L, Schlossman S, Duke-Cohan J. Biochemical and genetic studies of pigment-type switching. Pigment Cell Res. 2000;13 Suppl 8:48–53.

28. Ollmann MM, Wilson BD, Yang YK, Kerns JA, Chen Y, Gantz I, et al. Antagonism of central melanocortin receptors in vitro and in vivo by agouti-related protein. Science. 1997 Oct 3;278(5335):135–8.

29. 2iqr » Melanocortin-4 receptor model (active state) with agonist NDP-MSH - Orientations of Proteins in Membranes (OPM) database [Internet]. [cited 2016 Dec 3]. Available from: http://opm.phar.umich.edu/protein.php?pdbid=2iqr

30. Pogozheva ID, Chai B-X, Lomize AL, Fong TM, Weinberg DH, Nargund RP, et al. Interactions of human melanocortin 4 receptor with nonpeptide and peptide agonists. Biochemistry (Mosc). 2005 Aug 30;44(34):11329–41.

31. Skin Cancer - Melanoma | American Cancer Society [Internet]. [cited 2016 Dec 1]. Available from: http://www.cancer.org/cancer/skincancer-melanoma/

32. Huang Z -m., Chinen M, Chang PJ, Xie T, Zhong L, Demetriou S, et al. Targeting protein-trafficking pathways alters melanoma treatment sensitivity. Proc Natl Acad Sci. 2012 Jan 10;109(2):553–8.

33. Chen KG, Leapman RD, Zhang G, Lai B, Valencia JC, Cardarelli CO, et al. Influence of melanosome dynamics on melanoma drug sensitivity. J Natl Cancer Inst. 2009 Sep 16;101(18):1259–71.

34. Craik DJ, Fairlie DP, Liras S, Price D. The Future of Peptide-based Drugs. Chem Biol Drug Des. 2013 Jan 1;81(1):136–47.

35. Fosgerau K, Hoffmann T. Peptide therapeutics: current status and future directions. Drug Discov Today. 2015 Jan;20(1):122–8.

36. Dharanipragada R. New modalities in conformationally constrained peptides for potency, selectivity and cell permeation. Future Med Chem. 2013 May 1;5(7):831–49.

37. Piekielna J, Perlikowska R, Gach K, Janecka A. Cyclization in Opioid Peptides. Curr Drug Targets. 2013 Jun 1;14(7):798–816.

CHAPTER 2
STRUCTURAL MUTATIONS OF AGOUTI SIGNALING PEPTIDE

ASIP and Melanoma

The pigment eumelanin provides a vital first defense against UV damage. Melanosomes are organelles in melanocytes that synthesize eumelanin and shuttle it to nearby basal cells. In melanoma, a skin cancer that arises from unregulated melanocyte proliferation, the natural eumelanin distribution works against treatment of this cancer with standard chemotherapy. Melanosomes sequester and even transfer chemotherapeutics, such as cisplatin and dacarbazine, outside of the cell. Consequently, the chemotherapeutic agent cannot effectively reach the nucleus, an essential step for crosslinking DNA and initiating the apoptosis pathway. For this reason, melanoma is especially resistant to traditional chemotherapy and causes the majority of skin cancer deaths. The American Cancer Society estimates that 76,380 new melanomas will be diagnosed and over 10,000 people will die of melanoma in the US in 2016 (1).

Huang et al. demonstrated that pretreating melanoma cells in culture with agouti signaling peptide (ASIP) greatly enhances small molecule inhibitor based chemotherapeutic agents (2). Specifically, the survival of melanoma cells in culture is reduced two- to three-fold. This enhancement of chemotherapeutic action is thought to arise from two important downstream consequences of ASIP action. First, ASIP reduces melanosome formation, preventing sequestration and thus increasing the intracellular chemotherapeutic concentration. Second, ASIP impairs proper melanosome function by limiting protein trafficking to the organelles, further decreasing inadvertent absorption of chemotherapy agents by melanosomes (2).

Based on these results, ASIP offers great potential for improving the efficacy of melanoma chemotherapy. ASIP co-administration would likely require lower doses of toxic chemotherapeutics, while at the same time, improving chemotherapeutic action. ASIP, being a normal protein found in skin, is non-toxic and is anticipated to have minimal side effects. The goal of this work is to improve ASIP potency by increasing its affinity and specificity to its cognate, melanocortin receptor 1 (MC1R).

ASIP 2K

Motivation

ASIP 2K describes a mutant with 2 lysine residues placed outside of the Cys-rich region of ASIP-YY. This positively charged mutation was motivated by the β-defensin electrostatic binding scheme. β-defensins are small peptides with 3 disulfide bridges and large patches of positive charge. Nix et al. concluded that human β-defensin 3 binds to the negative binding pocket of human MC1R using these patches of positive charge, rather than using a specific amino acid sequence (3).

A

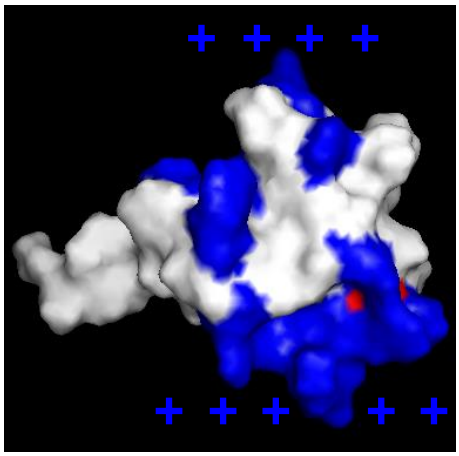

B

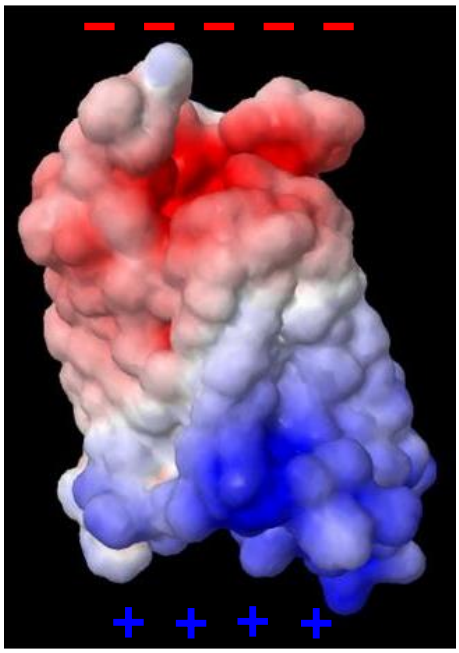

Figure 2.1. Molecular Models for HBD3 and MC1R
(A) The model of human β-defensin 3 has positively charged residues (blue) in two patches. (B) An electrostatic potential model of melanocortin receptor 1 with the negatively charged extracellular binding pocket (red) and positive cytosolic region (blue). Adapted from Nix et al (3).

We hypothesized that employing similar electrostatic interactions could increase the binding between ASIP and MC1R. We placed the 2 positive charges just outside of

the disulfide-rich structured region of ASIP, near the random-coil N-terminus, hypothesizing that these additional positive charges would interact with the negative binding pocket of MC1R, increasing the overall binding of the peptide to the receptor.

A

KKVVRPRTPLSAPCVATRNSCKPPAPACCDPCASCYCRFFRSACYCRVLSLNC
KKVVRPRTPLKKPCVATRNSCKPPAPACCDPCASCYCRFFRSACYCRVLSLNC

B

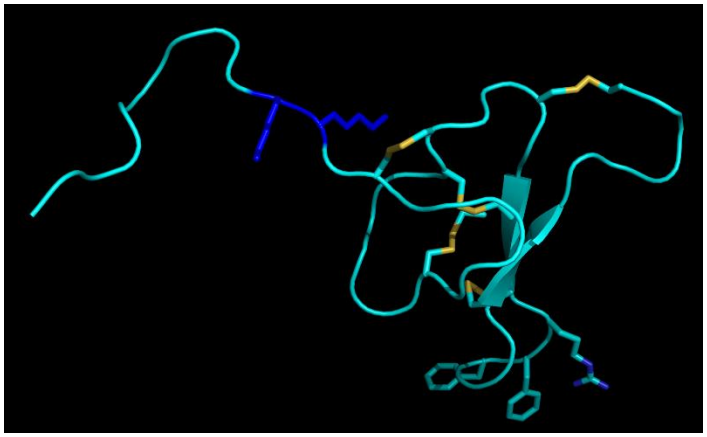

Figure 2.2. Sequence Alterations and Model for ASIP 2K
(A) The first line is a portion of the native ASIP sequence with Q115Y/S124Y, known as ASIP-YY. The second sequence shows the placement of two lysine mutations (underlined) immediately before the structured region of the protein. (B) Model of ASIP 2K (cyan) with the two lysine mutations (blue) proximal to the structured domain. This change was designed to be distant from the binding motif Arg-Arg-Phe (stick representation).

Similar to ASIP controlling eumelanin production through MC1R, the homologous agouti-related peptide (AgRP) affects feeding behavior by acting on MC4R in neurons (4). In work done by Madonna et al., AgRP 2K similarly describes a mutant with 2 lysine residues placed outside of the Cys-rich region of AgRP (5). This work also found that adding positive charge to non-ICK regions of AgRP proportionally increased long term feeding in rats. In contrast to ASIP 2K's proposed method for

increased binding, the positively charged AgRP mutations increased the efficacy of the peptide through interactions with glycosaminoglycan molecules affixed to neuronal cell membranes (6). This phenomenon does not occur with ASIP acting on melanocytes.

Methods

Peptide Synthesis and Cleavage Conditions

We used the standard ASIP-YY methods for ASIP 2K, as described in McNulty et al (7). The peptide was synthesized on a Liberty 1 Peptide Synthesizer from CEM Corporation, fitted with a Discover Microwave unit, using Fmoc chemistry. The use of H-rink amide ChemMatrix resin resulted in an amidated C-terminus. Fmoc deprotection was achieved with 20% piperidine solution in DMF. All amino acids were double coupled with microwave cycles using 4 equivalents of Fmoc-amino acid in HOBt/DIC, and arginine couplings included an extended coupling. Coupling cycles concluded with a capping step using 10% acetic anhydride in DMF. The peptide was acetylated at the N-terminus by reacting with the same acetic anhydride solution for 5 minutes. Fully synthesized peptide resins were split into four reaction vessels, washed with DCM, and dried.

ASIP 2K was cleaved using a cocktail consisting of 10 mL TFA, 0.3 mL TIPS, 0.3 mL EDT, and 0.15 mL phenol. The resin was filtered and washed with 1 mL TFA. The combined filtrate and wash was put under a stream of nitrogen gas to evaporate the TFA. After the total volume was reduced to 5 mL, it was then added to 45 mL of

cold dry diethyl ether for precipitation. The precipitate was collected by centrifugation, and the ether was discarded. After a second wash with ether, the pelleted protein was dissolved in 10 mL 2:1 H_2O/ACN (0.06% TFA). The volume was doubled with buffer A (0.06% TFA in water) and immediately purified by reverse phase HPLC on Vydac preparative C18 columns. Collected fractions were analyzed by ESI-MS on a Micromass ZMD mass spectrometer. Peptides corresponding to the correct molecular weight were pooled together and lyophilized.

Oxidative Folding

ASIP 2K was stirred at room temperature for 27 hours in a buffer consisting of 1.6 M guanidine, 100 mM tris, 5 mM reduced glutathione, 0.5 mM oxidized glutathione, and 10% DMSO, at pH 7.9. Peptide concentration was typically 0.1 mg/mL. Folded peptides were purified using RP-HPLC on C18 semi-preparative columns. Via mass spectrometry, we confirmed a mass loss of 10 Da indicating the formation of 5 disulfide bonds. We used NEM to verify that there were no free cysteines. The purity of folded peptide was checked using analytical columns on a Shimadzu HPLC machine. Peptide quantification was done using UV absorption.

Competitive Binding Assay

Through our collaboration with Christopher Kaelin in the Barsh Group at Stanford University, ligand binding assays were performed using the DELPHIA europium-based quantification system on human embryonic kidney (HEK) 293T cells transiently transfected with a MC1R construct, as described in Candille et al (8).

Briefly, cells are incubated with excess europium labeled, 4-norleucine, 7-D-phenylalanine alpha melanocyte stimulating hormone (Eu-NDP-MSH). Varied amounts of antagonist are added, displacing some of the bound Eu-NDP-MSH. A wash step removes unbound NDP-MSH and the remaining europium signal is measured as fluorescence using the DELPHIA system.

Binding Results

ASIP 2K had reduced binding to MC1R (see Figure 2.6). The competitive binding assay showed ASIP 2K binds with a Ki of 5.560 nM, which is roughly two times the Ki for ASIP-YY (2.398 nM). Due to these poor pharmacology results, we did not pursue additional experiments.

ASIP S129V/N131L Double Mutant

Motivation

Highly specific binding to MC1R is necessary for the utility of ASIP as a therapeutic. Non-specific binding would lead to a multitude of side effects and decrease the efficiency of ASIP. While both ASIP and AgRP bind tightly to MC4R, only ASIP binds to MC1R (4). Patel et al. describes chimera studies of ASIP and AgRP, elucidating which factors mediate binding to MC1R (9). This work showed that the C-terminus of ASIP is necessary for inverse agonist activity at MC1R. Patel hypothesized that the hydrophobic residues in the C-terminal loop of ASIP coordinated with the first extracellular loop of MC1R. The C-terminal loop of ASIP is fundamental to increasing the specificity for MC1R. Molecular modeling indicates

that there are two possible mutations in the C-terminal loop that could increase that hydrophobic interaction. All molecular modeling utilized the Mosberg model of ASIP bound to MC1R, obtained from http://mosberglab.phar.umich.edu/resources/ (10). Each substituted amino acid was designed to be similar in size to the original residue, to prevent side chain clashes or the formation of unfavorable cavities. Serine at position 129 was replaced with valine and asparagine at position 131 was replaced with leucine. According to modelling, these new side chains remain in close proximity to the receptor (see Figure 2.3).

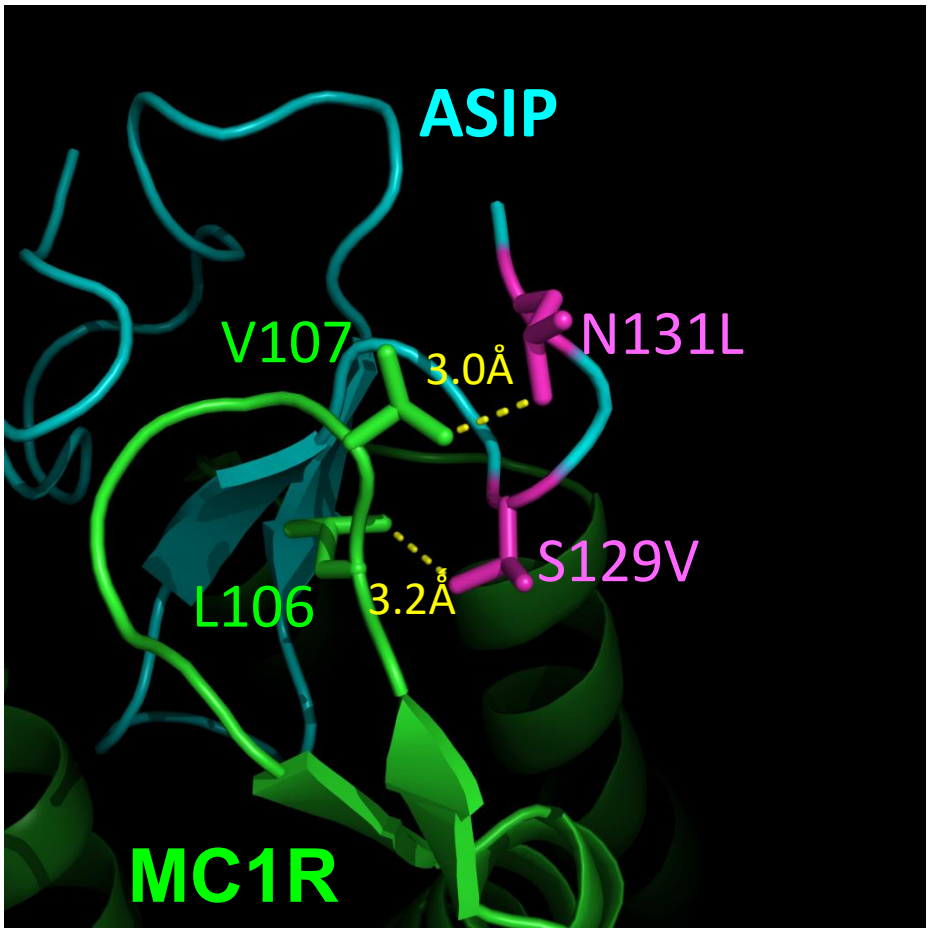

Figure 2.3. ASIP S129V/N131L Bound to MC1R
In the foreground is extracellular loop 1 of melanocortin receptor 1 (green). ASIP (cyan) has two hydrophobic mutations (pink) in the C-terminal loop. These are within 3.2 angstroms of the two hydrophobic residues from MC1R that are represented with sticks and labelled.

Methods

Peptide Synthesis and Cleavage Conditions

The double mutant was synthesized in the same manner described for ASIP 2K. To reduce undesired t-butylation, we used a modified cleave cocktail consisting of 15 mL TFA, 1 mL TIPS, 2 mL EDT, and 1 mL phenol for one quarter of a 0.10 mmol

synthesis. The resin was filtered and washed with 10 mL TFA. The combined filtrate and wash was put under a stream of nitrogen gas to evaporate the TFA. After the total volume was reduced to 5 mL, it was then added to 45 mL of cold dry diethyl ether for precipitation. The precipitate was collected by centrifugation, and the ether was discarded. After a second wash with ether, the pelleted protein was dissolved in 20 mL 1:1 H_2O/ACN (0.06% TFA) and lyophilized.

Lyophilized peptide was brought to a concentration of 0.1 mg/mL using 1:1 H_2O/ACN (0.06% TFA). This equilibrated at room temperature for a minimum of 15 minutes before the volume was quadrupled with buffer A (0.06% TFA in water). The sample was purified by reverse phase HPLC on Vydac preparative C18 columns, using extended methods to account for the delayed retention times of hydrophobic mutants.

Collected fractions were analyzed by ESI-MS on a Micromass ZMD mass spectrometer. Peptides corresponding to the correct molecular weight were pooled together and lyophilized. Fractions containing only irreversible +51 Da adducts were discarded. Peptide modified by a t-butyl group, resulting in a mass increase of 56 Da, was treated with 300 equivalents of DMSO in TFA for 1 hour. Peptide concentration was typically 0.2 mg/mL. The protein was collected using ether precipitation and lyophilized. Reducing this sample, using 20mM DTT in 20mM tris (pH 7.4) at 37°C for no more than one hour, gave unfolded ASIP without t-butylation. Attempts to reduce ASIP at 37°C for longer than one hour resulted in the unfolded peptide irreversibly precipitating.

Oxidative Folding

ASIP S129L/N131L was oxidatively folded using the same buffer as ASIP-YY (1.6 M guanidine, 100 mM tris, 5 mM reduced glutathione, 0.5 mM oxidized glutathione, and 10% DMSO, at pH 7.9). A single folded peak was not apparent within 7 days of starting the fold reaction, testing every 24 hours. Mass spectrometry data suggests that less than 5% of the peptide had a 10 Da decrease, which would indicate a fully folded peptide. Due to this prohibitively low folding yield, this double mutant was not pursued in subsequent experiments, including the competitive binding assay.

ASIP S129L and N131L

Motivation

The S129L and N131L mutations are also based on the conclusion drawn by Patel et al., that the C-terminal loop is necessary for inverse agonism because it interacts with the hydrophobic extracellular loop of MC1R (9). By increasing the hydrophobic patch on the C-terminal loop, we hypothesized that the specificity of ASIP for MC1R would be enhanced. The double mutant S129V/N131L failed due to low solubility; two separate single mutations would each be less hydrophobic and therefore fold more completely in aqueous conditions. ASIP S129V failed to synthesize and was modified to S129L.

A

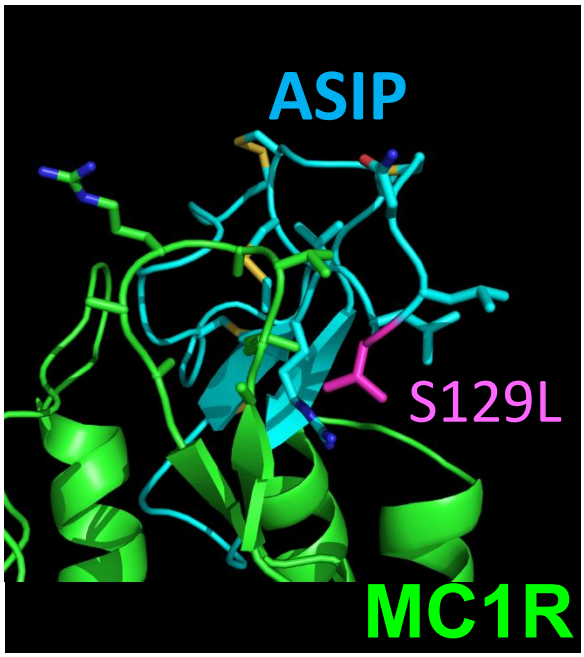

B

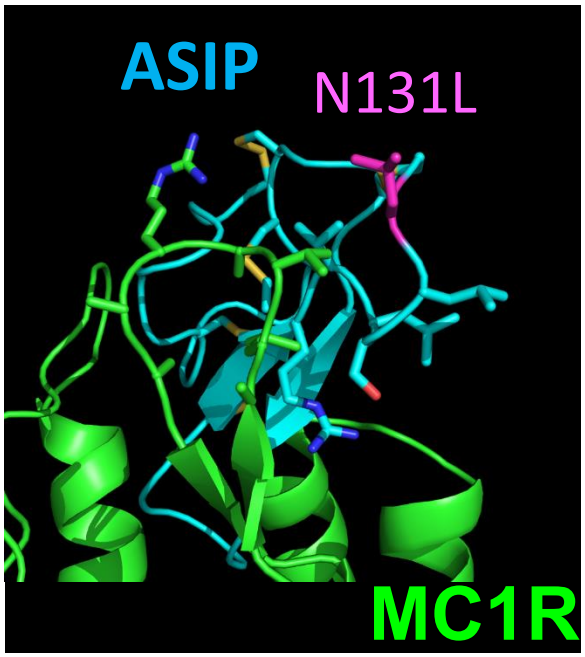

Figure 2.4. ASIP S129L Bound to MC1R
In the foreground is extracellular loop 1 of melanocortin receptor 1 (green). ASIP (cyan) is shown with the disulfide bridges (yellow) and one hydrophobic mutation (pink) in the C-terminal loop. (A) depicts S129L and (B) shows N131L. These mutations could possibly interact with several hydrophobic residues from MC1R that are represented with sticks.

Methods

Peptide Synthesis and Cleavage Conditions

ASIP S129L and N131L were synthesized as described in previous sections. To reduce undesired t-butylation, we used a modified cleave cocktail consisting of 15 mL TFA, 1 mL TIPS, 2 mL EDT, and 1 mL phenol for one quarter of a 0.10 mmol synthesis. The resin was filtered and washed with 10 mL TFA. The combined filtrate and wash was put under a stream of nitrogen gas to evaporate the TFA. After the total volume was reduced to 5 mL, it was then added to 45 mL of cold dry diethyl ether for precipitation. The precipitate was collected by centrifugation, and the ether was discarded. After a second wash with ether, the pelleted protein was dissolved in 20 mL 1:1 H_2O/ACN (0.06% TFA) and lyophilized.

Lyophilized peptide was brought to a concentration of 0.1 mg/mL using 1:1 H_2O/ACN (0.06% TFA). This equilibrated at room temperature for a minimum of 15 minutes before the volume was quadrupled with buffer A (0.06% TFA in water). The sample was purified by reverse phase HPLC on Vydac preparative C18 columns, using extended methods, to account for the delayed retention times of hydrophobic mutants.

Collected fractions were analyzed by ESI-MS on a Micromass ZMD mass spectrometer. Peptides corresponding to the correct molecular weight were pooled together and lyophilized. Fractions containing only irreversible +51 Da adducts were discarded. Peptide modified by a t-butyl group, resulting in a mass increase of 56 Da,

was treated with 300 equivalents of DMSO in TFA for 1 hour. Peptide concentration was typically 0.2 mg/mL. The protein was collected using ether precipitation and lyophilized. Reducing this sample, using 20mM DTT in 20mM tris (pH 7.4) at 37°C for no more than one hour, gave unfolded ASIP without t-butylation. Attempts to reduce ASIP at 37°C for longer than one hour resulted in the unfolded peptide irreversibly precipitating.

Oxidative Folding

Purified peptide was incubated at a concentration of 0.1 mg/mL in the original folding buffer (1.6 M guanidine, 100 mM tris, 5 mM reduced glutathione, 0.5 mM oxidized glutathione, and 10% DMSO, at pH 7.9) at 4°C for 72 hours. This differs from ASIP-YY, which is folded by stirring at room temperature for 27 hours.

The misfolded peptide and glutathione adducts from the fold reaction were collected and reduced using 20 mM DTT in 20 mM tris (pH 7.4) at 37°C for no more than one hour. The resulting unfolded peptide was lyophilized, quantified and folded again. Sufficient quantities of peptide were produced using this iterative process.

Competitive Binding Assay

The binding evaluation was performed in the same manner as ASIP 2K. Through our collaboration with Christopher Kaelin in the Barsh Group at Stanford University, ligand binding assays were performed using the DELPHIA europium-based quantification system on human embryonic kidney (HEK) 293T cells transiently transfected with a MC1R construct.

Binding Results

ASIP S129L and ASIP N131L also had reduced binding to MC1R (see figure 2.6). The binding assay showed ASIP S129L binds with a Ki of 9.355 nM, nearly four times the Ki for ASIP-YY (2.398 nM). ASIP N131L binds with a Ki of 92.48 nM, approximately forty times the Ki for ASIP-YY. Due to these poor pharmacology results, we did not pursue additional experiments for either mutant.

Computational Mutations of the C-terminus

Motivation

Patel et al. demonstrated that chimera peptides require ASIP's C-terminal loop to act as an inverse agonist at MC1R and hypothesized that ASIP's C-terminal loop interacts with the first extracellular loop of MC1R (9). Previous sections of this chapter described experiments utilizing rational design to increase the known hydrophobic interactions between the two proteins. Computational modeling is another route to designing mutations on the C-terminal loop.

Methods

Computational Design

Beau Norgeot completed the computational design portion of this project. Briefly, he designed sequences using the Seq-Tol design algorithm on the ROSIE (Rosetta Online Server that Includes Everyone) server supported by the Gray Lab at Johns

Hopkins University. He limited mutations to the 6 amino acids in the C-terminal loop, rather than allowing the algorithm to change all residues in the peptide.

To score the designed sequences, he used Docking2 protocol on the ROSIE server. The Mosberg model was obtained from http://mosberglab.phar.umich.edu/resources/ and used as an approximation for correct binding (10). A lower energy output from the docking software would indicate a beneficial change in the sequence. Computational alanine scanning, which generates docking score differences when each amino acid was replaced with an alanine, was incorporated into this score. If replacing the residue in the designed sequence resulted in a larger decrease in score than replacing it in the native sequence, then the designed sequence was considered superior. Lastly, he designed the final sequence based on residue frequency at each position.

A

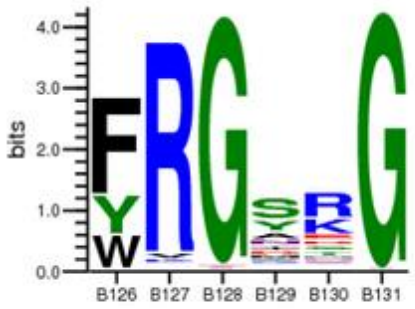

B

```
KKVVRPRTPLSAPCVATRNSCKPPAPACCDPCASCYCRFFRSACYCRVLSLNC
KKVVRPRTPLSAPCVATRNSCKPPAPACCDPCASCYCRFFRSACYCFRGSRGC
```

Figure 2.5. Relative Residue Output per Position and Final Computational Mutant Sequence

(A) Along the abscissa is the residue position, while the ordinate is the frequency of that residue being placed at that position. Larger letters are the most frequent (126-128 and 131), while smaller letters have more variation at that position. (B) The ASIP-YY sequence is compared to the computational mutant, with changes to the C-terminus underlined.

The resulting sequence has reasonable modifications. The arginine residue is shifted from position 126 to 127 and the serine stays at position 129. However, the glycine residues may be an artifact of this process, as the conformational freedom of glycine residues skews the energy scores given by the Rosetta suite of programs. The extra flexibility allows for more ideal geometry, which is a component of the score. However, the glycine residues in ASIP's C-terminal loop do not directly interact with MC1R, and therefore do not improve the interface between the C-terminal loop and the first extracellular loop of MC1R.

Peptide Synthesis and Folding

We completed the peptide synthesis, folding, and purification together. We used the same methods as applied to ASIP 2K. This peptide was cleaved using a cocktail consisting of 10 mL TFA, 0.3 mL TIPS, 0.3 mL EDT, and 0.15 mL phenol. Following ether precipitation and purification using RP-HPLC, the computational mutant was oxidatively folded at room temperature for 27 hours in a buffer consisting of 1.6 M guanidine, 100 mM tris, 5 mM reduced glutathione, 0.5 mM oxidized glutathione, and 10% DMSO, at pH 7.9. Peptide concentration was typically 0.1 mg/mL.

Competitive Binding Assay

The binding evaluation was performed in the same manner as ASIP 2K. Through our collaboration with Christopher Kaelin in the Barsh Group at Stanford University, ligand binding assays were performed using the DELPHIA europium-based quantification system on human embryonic kidney (HEK) 293T cells transiently transfected with a MC1R construct.

Binding Results

The computational mutant also had reduced binding at MC1R (see Figure 2.6). The binding assay showed this mutant binds with a Ki of 34.44 nM, which is roughly fourteen times the size of the Ki for ASIP-YY, 2.398 nM. Due to these poor pharmacology results, we did not pursue additional experiments.

A

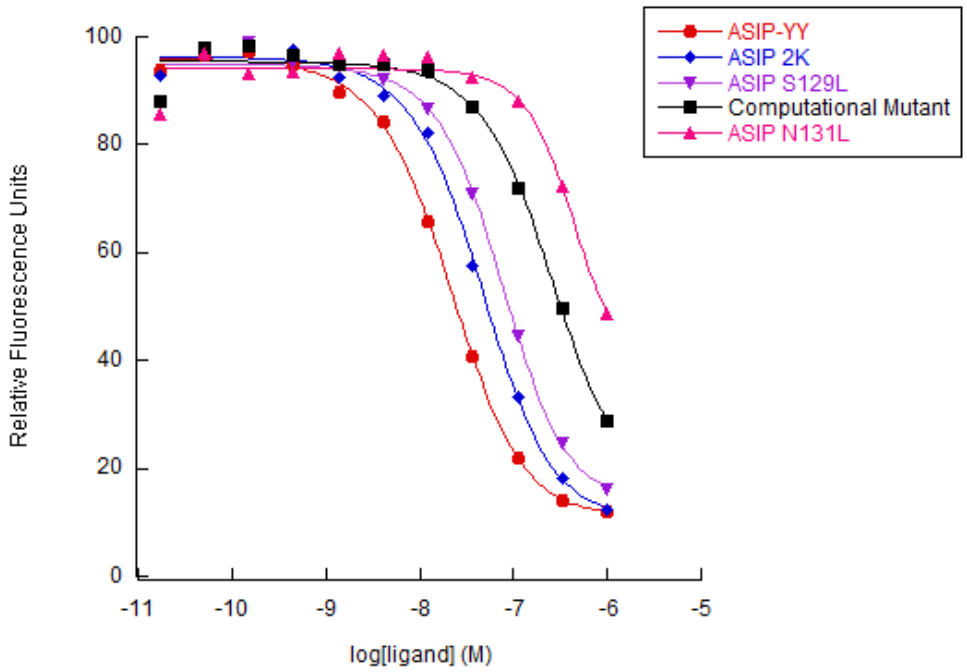

B

Peptide	n	Ki (nM)	SEM
ASIP-YY	5	2.398	0.2022
ASIP 2K	3	5.560	0.2883
ASIP S129L	3	9.355	1.677
Computational Mutant	3	34.44	1.823
ASIP N131L	2	92.48	20.23

Figure 2.6. Binding Curves and Ki Values for All Mutants
(A) Competition binding curves comparing all mutants. The logarithm of antagonist is plotted on the abscissa while the amount of Eu-NDP-MSH bound, measured as relative fluorescence, is plotted on the ordinate. (B) Mean Ki values (in nM) were calculated by fitting the data to a sigmoidal, dose-response curve with variable slope. Standard error of the mean (SEM) is listed for each peptide.

Discussion

Via evolution, ASIP became a high-affinity binding partner for MC1R. The discussed modifications unfortunately did not improve receptor binding properties over wild-type. The Ki values for ASIP 2K and ASIP S129L are within an order of magnitude of the Ki for ASIP-YY. These mutants still bind tightly to MC1R, just not with as high affinity as the native sequence.

Although these changes did not make ASIP more effective as a therapeutic, these projects showed new aspects of the interaction between ASIP and MC1R. We added positive charge in the form of lysine residues outside of the cysteine rich region. We hypothesize this had a neutral impact because this area is also near the positively charged lysine/arginine rich region of ASIP. All of the hydrophobic sequences decreased binding affinity. This could indicate that the C-terminus of ASIP and the first extracellular loop of MC1R have ideal complementarity. Additional hydrophobicity is unnecessary and detrimental to this interaction. Lastly, we can use the failure of the first computational mutant to guide future iterations of computational design. For example, we can slightly lower the impact of bond geometry on the overall energy score.

We also gained new protocols for cleaving, purifying, and folding ASIP-YY or future hydrophobic mutants. ASIP-YY yields were low for several reasons, including adducts after cleaving the peptide from the resin, inadequate precipitation in the ether precipitation step, low solubility for the unfolded peptide, and low folding yields.

Due to side reactions, some of the crude ASIP-YY had covalent adducts. It became necessary to address these adducts because more than 50% of the hydrophobic mutants of ASIP was in the form of a +51 Da adduct or +56 Da adduct, corresponding to an irreversible piperidine adduct and a t-butyl group attached to a cysteine, respectively.

Lukszo et al. suggests that the +51 Da adduct is due to using piperidine to deprotect a C-terminal cysteine (11). The steric freedom from being on the terminus allows the piperidine to covalently attach to the β carbon of the cysteine, creating a 3-(1-piperidinyl)alanine. The mutants and ASIP-YY all have a C-terminal cysteine and piperidine is used to deprotect during peptide synthesis. However, there is a minor amount of the +51 Da adduct for cyclic ASIP, which is synthesized with a C-terminal alanine (see Chapter 3). Two cases are possible: a different adduct is also causing +51 Da or all of the +51 Da adduct could be caused by something other than a C-terminal 3-(1-piperidinyl)alanine. Casting further doubt, Lukszo et al. did not see any adduct formation in small peptides when the cysteine was protected with a trityl group, as it is in ASIP (11). Using piperazine instead of piperidine during peptide synthesis could elucidate if piperidine is causing the +51 Da adduct. If the conversion to 3-(1-piperidinyl)alanine is responsible for this adduct, then it is irreversible. Additional washes with pure TFA, incubation in reducing conditions, or incubation with DMSO all failed to decrease the amount of +51 Da adduct. However, it is possible to purify away this adduct using reverse phase HPLC.

For the +56 adduct, we confirmed the t-butyl group was on a cysteine using several methods. During synthesis, we use t-butyl as a protecting group for serine, threonine and tyrosine. The protectant group is removed under acidic conditions (TFA). Free t-butyl groups from these three amino acids reacted with cysteine residues during the cleave step. Subsequent treatments with TFA does not reduce the amount of +56 adduct, indicating that serine, threonine, and tyrosine were not t-butylated. Verifying this result, NEM tests indicated that the +56 Da adduct only had 9 free thiol groups, although 10 cysteines are in the ASIP-YY sequence. As almost 20% of the amino acids in this peptide are cysteines, it follows that a portion of the cysteine residues would acquire aberrant t-butylation even in the presence of scavengers.

To reduce this undesirable t-butylation, we modified the acid solution used to remove the protecting groups and cleave the peptide from the resin. In the modified cocktail, increased concentrations of scavengers were used: 79% TFA / 5% TIPS / 11% EDT / 5% phenol, increased from 93% TFA / 3% TIPS / 3% EDT / 1% phenol. Another strategy is to dilute the t-butyl groups by increasing the overall volume of the cleavage cocktail, inspired by the method in Madonna et al. for working with AgRP (5). The Madonna et al. cocktail contains: 15 mL TFA, 1 mL TIPS, 0.5 mL EDT, and 0.5 mL phenol for one half of a 0.10 mmol synthesis. The final cocktail for ASIP was: 15 mL TFA, 1 mL TIPS, 2 mL EDT, and 1 mL phenol for one quarter of a 0.10 mmol synthesis.

It was necessary to alter this method to successfully precipitate the protein. Increasing the concentration of the scavengers and increasing the total volume caused lower

protein concentrations. Attempts to ether precipitate the dilute protein resulted in either no protein precipitation or a very small protein pellet. To overcome this, streams of nitrogen were used to evaporate excess TFA until the total volume was less than 5 mL. The peptide yield increased significantly from evaporating off the TFA after treating the peptide with the modified cleave cocktail or the original cocktail. Both increasing the amount of scavenger and increasing the volume of cleavage cocktail only partially reduced the amount of adducts. However, this technique increased the overall yield of ASIP from a given amount of resin and therefore used for ASIP-YY, all hydrophobic mutants, and cyclic ASIP (see Chapter 3).

After ether precipitation, the peptide was purified using reverse phase HPLC. The fractions containing a +56 Da adduct were pooled and this remaining t-butylation was removed chemically. This +56 Da adduct is referenced in Patel et al. as an irreversible t-butylation during long cleave reactions (9). Due to our previous experience with orthogonal protection of β-defensin cysteines, we had several methods available to remove t-butyl groups from cysteines. During orthogonal protection, two specific cysteines in the β-defensin are protected with a t-butyl group. Each step in the oxidative folding removes one set of protecting groups, ensuring that the correct connectivity is formed, one disulfide pair at a time. Removing the t-butyl from ASIP requires less rigorous methods than orthogonally folding β-defensins because forming the correct disulfide connectivity is not necessary while removing the t-butyl groups. The method that had the highest efficiency for removing t-butyl groups from the

cysteines in ASIP had been abandoned in the β-defensin project due to low folded β-defensin yields. After removing the t-butyl groups using DMSO and TFA, the sample was partially oxidized. The protein was collected using ether precipitation and lyophilized. Reducing this sample gave unfolded ASIP without t-butylation.

These projects also highlighted new methods for increasing the solubility of unfolded peptide. Predictably, the unfolded hydrophobic mutants were less soluble than ASIP-YY. To combat this, we used increased volumes of buffer with proportionally more acetonitrile. ASIP-YY is optimally solubilized in 2:1 water to acetonitrile. The hydrophobic mutants were optimally solubilized in 1:1 water to acetonitrile. Increased time to fully dissolve was also necessary. Before adding more water, which is needed to dilute the acetonitrile before running the sample on a reverse phase column, we let the peptide equilibrate for a minimum of 15 minutes in the optimal buffer ratio. We also needed extended methods, to account for the delayed retention times of hydrophobic mutants. These methods will facilitate working with new hydrophobic mutants and elucidate techniques that can be applied to ASIP-YY.

In order to fold the hydrophobic mutants, we attempted a number of different oxidative folding techniques. Changes to the fold buffer, including varying the DMSO concentration, altering the glutathione concentration, or using 50% isopropanol to mitigate low solubility, resulted in inadequate fold yields. The optimal method, utilizing low temperatures to slow the fold reaction, was inspired by Wu et al (12). The highest fold yield was from incubating 0.1 mg/mL peptide in the original

folding buffer at 4°C for 72 hours. This differs from ASIP-YY, which is folded by stirring at room temperature for 27 hours.

Lastly, poor folding yields forced us to address methods for recovering misfolded peptide. While the majority of ASIP-YY does fold into a dominant species, a small amount will form glutathione adducts. ASIP will not fold into one species in the absence of glutathione. For the hydrophobic mutants, the majority of the protein forms glutathione adducts. The misfolded peptide and glutathione adducts from the fold reaction were collected and reduced. The resulting unfolded peptide was lyophilized, quantified and folded again. This iterative process dramatically increased the amount of folded peptide from each synthesis. Most of these techniques can be applied to ASIP-YY, increasing the yield of this difficult protein.

References

1. Key statistics for melanoma skin cancer [Internet]. [cited 2016 Dec 1]. Available from: http://www.cancer.org/cancer/skincancer-melanoma/detailedguide/melanoma-skin-cancer-key-statistics

2. Huang Z -m., Chinen M, Chang PJ, Xie T, Zhong L, Demetriou S, et al. Targeting protein-trafficking pathways alters melanoma treatment sensitivity. Proc Natl Acad Sci. 2012 Jan 10;109(2):553–8.

3. Nix MA, Kaelin CB, Ta T, Weis A, Morton GJ, Barsh GS, et al. Molecular and Functional Analysis of Human β-Defensin 3 Action at Melanocortin Receptors. Chem Biol. 2013 Jun;20(6):784–95.

4. Abdel-Malek ZA. Melanocortin receptors: their functions and regulation by physiological agonists and antagonists. Cell Mol Life Sci CMLS. 2001 Mar;58(3):434–41.

5. Madonna ME, Schurdak J, Yang Y-K, Benoit S, Millhauser GL. Agouti-related protein segments outside of the receptor binding core are required for enhanced short- and long-term feeding stimulation. ACS Chem Biol. 2012 Feb 17;7(2):395–402.

6. Reizes O, Clegg DJ, Strader AD, Benoit SC. A role for syndecan-3 in the melanocortin regulation of energy balance. Peptides. 2006 Feb;27(2):274–80.

7. McNulty JC, Jackson PJ, Thompson DA, Chai B, Gantz I, Barsh GS, et al. Structures of the agouti signaling protein. J Mol Biol. 2005 Mar 4;346(4):1059–70.

8. Candille SI, Kaelin CB, Cattanach BM, Yu B, Thompson DA, Nix MA, et al. A B-defensin mutation causes black coat color in domestic dogs. Science. 2007 Nov 30;318(5855):1418–23.

9. Patel MP, Cribb Fabersunne CS, Yang Y, Kaelin CB, Barsh GS, Millhauser GL. Loop-Swapped Chimeras of the Agouti-Related Protein and the Agouti Signaling Protein Identify Contacts Required for Melanocortin 1 Receptor Selectivity and Antagonism. J Mol Biol. 2010 Nov;404(1):45–55.

10. Chai B-X, Pogozheva ID, Lai Y-M, Li J-Y, Neubig RR, Mosberg HI, et al. Receptor−Antagonist Interactions in the Complexes of Agouti and Agouti-Related Protein with Human Melanocortin 1 and 4 Receptors † , ‡. Biochemistry (Mosc). 2005 Mar;44(9):3418–31.

11. Lukszo J, Patterson D, Albericio F, Kates SA. 3-(1-Piperidinyl)alanine formation during the preparation ofC-terminal cysteine peptides with the Fmoc/t-Bu strategy. Lett Pept Sci. 1996 Jul;3(3):157–66.

12. Wu X, Wu Y, Zhu F, Yang Q, Wu Q, Zhangsun D, et al. Optimal Cleavage and Oxidative Folding of α-Conotoxin TxIB as a Therapeutic Candidate Peptide. Mar Drugs. 2013 Sep 17;11(9):3537–53.

CHAPTER 3
CYCLIZATION OF AGOUTI SIGNALING PEPTIDE

Motivation

The use of peptides as therapeutics or scaffolds to deliver therapeutic payloads or imaging agents has become increasingly popular in recent years. Peptides offer high levels of specificity and potency to their molecular targets (1,2). The drawbacks that come with the use of peptides over small molecules include reduced absorption, necessitating intravenous injection in most cases, and a high susceptibility to proteases (3,4). The effort to improve peptide stability has led to interest in knottin peptides, commonly observed in nature in plants and invertebrate toxins, as highly stable scaffolds (5–7).

Knottin peptides are attractive scaffolds for medical purposes due to several desirable production and pharmaceutical qualities. Knottins can be produced in a variety of ways, either chemically or using recombinant methods, allowing for diverse modifications to be made. They are able to maintain their structure and function even after exposure to high temperature, extreme pH, and proteolytic enzymes (8–10). They are also tolerant to mutagenesis, maintaining their proper folding even when a variety of amino acids are substituted into the peptide for drug purposes. These characteristics are derived from an inhibitor cystine knot (ICK) core consisting of three disulfide bonds, one of which threads through the other two, conferring the peptide with exceptional stability (11). A similar motif is found in plant cyclotides where it is referred to as a cyclic cystine knot (CCK). Along with a conserved three-disulfide knot connectivity, cyclotides also possess a backbone N to C-terminal peptide bond. This backbone cyclization combined with the CCK core work

synergistically to make cyclotides especially resistant to thermal, chemical, and proteolytic degradation (12–15).

Motivated by these qualities of plant cyclotides, several groups have utilized cyclization of non-ICK peptides via chemical methods to successfully increase their stability and function (16,17). Cyclization renders peptides less susceptible to proteases, and may change the internal dynamics, creating a more rigid structure (18). Improvements of peptide folding have also been observed after cyclization of disulfide-rich peptides, presumably through a reduction in entropy of the unfolded state (19). The benefits of head-to-tail cyclization in knottin peptides have yet to be explored to the same degree and as it has in non-ICK peptides. In a few cases, cyclization has indeed yielded an improvement in the pharmaceutical properties of knottin peptides, though this is not true of every case (20–22). Designing knottin peptides to be more "cyclotide-like" may be a useful approach to facilitate drug design, and requires the exploration of the effects of cyclization on a diverse family of knottins.

One such family is the agouti family of knottins found in humans and other vertebrates (23). These peptides act as antagonists and inverse agonists of the melanocortin system, a group of G-protein-coupled receptors (GPCR) and ligands that modulate an array of physiological functions. Agouti-signaling peptide (ASIP) is involved in mammalian coat color and skin pigmentation through its interactions at melanocortin receptor 1 (MC1R) (24). Agouti-related peptide (AgRP) binds MC3R and MC4R in the hypothalamus, regulating energy expenditure and appetite (25–28).

Along with the three disulfide bonds forming the cystine knot, both peptides possess an additional two disulfide bonds, yielding three distinct and flexible loops that are important in melanocortin receptor binding and specificity.

ASIP, through its role in inhibiting melanosome production, has been identified as having a therapeutic role in augmenting the effects of chemotherapy treatments for melanoma (29). ASIP prevents the natural protein trafficking system in melanoma from sequestering and expelling chemotherapeutics. Therefore, less chemotherapy is needed for the same amount of cancer suppression. Adding stability to ASIP would improve its ability to enhance chemotherapy. As ASIP has therapeutic potential and already bears the ultra-stable ICK core, it is an ideal candidate for investigating the effects of cyclization on knottin peptides.

A

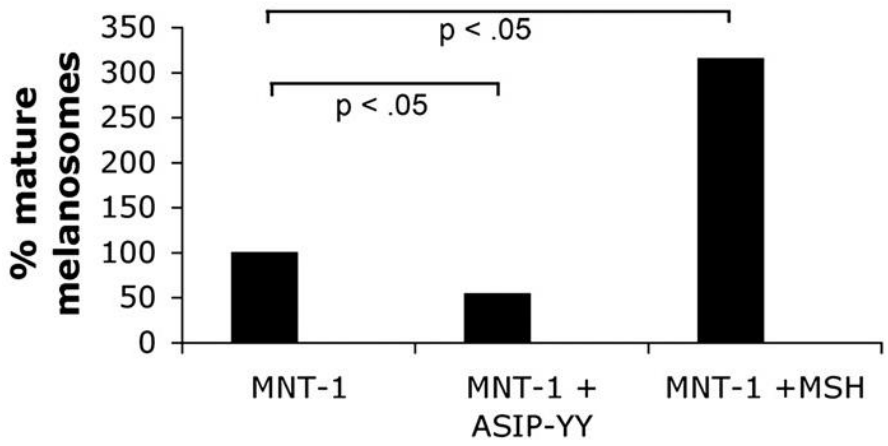

B

Treatment	Relative IC50	P value
cDDP alone	1	NA
cDDP with ASIP	0.3	<0.0001
DTIC alone	1	NA
DTIC with ASIP	0.5	<0.0001

Figure 3.1. ASIP as a Melanoma Treatment

(A) Human melanoma cells, named MNT-1 cells, have been treated with ASIP (middle bar), leading to a decrease in melanosomes compared to untreated cells (first bar). On the other hand, adding the agonist alpha melanocyte stimulating hormone (α-MSH) leads to a dramatic increase in melanosome production (last bar). This figure is reproduced from Huang et al (29). (B) When combined with ASIP, less of the chemotherapeutics known as *cis*-diaminedichloroplatinum II (cDDP) and dacarbazine (DTIC) are needed to kill 50% (IC50) of the cancer cells. These decreases are statistically significant. This table is altered from Huang et al (29).

Methods

Sequence Design

ASIP needed minimal alterations for cyclization. In order to have a N-terminal cysteine, we performed a circular permutation on the conventional sequence termed "ASIP-YY". Previous work in this lab determined that solubility is improved by including the naturally-occurring 13 amino acids prior to the first cysteine, while folding is greatly improved by the following point mutations: Q115Y, S124Y (30). Linear ASIP also uses this modified sequence. The 13 N-terminal amino acids in ASIP-YY seemed to perfectly bridge the gap between the first cysteine and the C-terminus in our molecular modeling.

After concluding we did not need an additional linker, we chose where peptide synthesis would begin. Of the 10 available cysteines, we chose C123 as the N-terminus because that left A122 as the C-terminus. Previous studies concluded that small, neutral amino acids work best as C-termini in native chemical ligation reactions (19).

A

KKVVRPRTPLSAPCVATRNSCKPPAPACCDPCASCYCRFFRSACYCRVLSLNC
CYCRVLSLNCKKVVRPRTPLSAPCVATRNSCKPPAPACCDPCASCYCRFFRSA

B

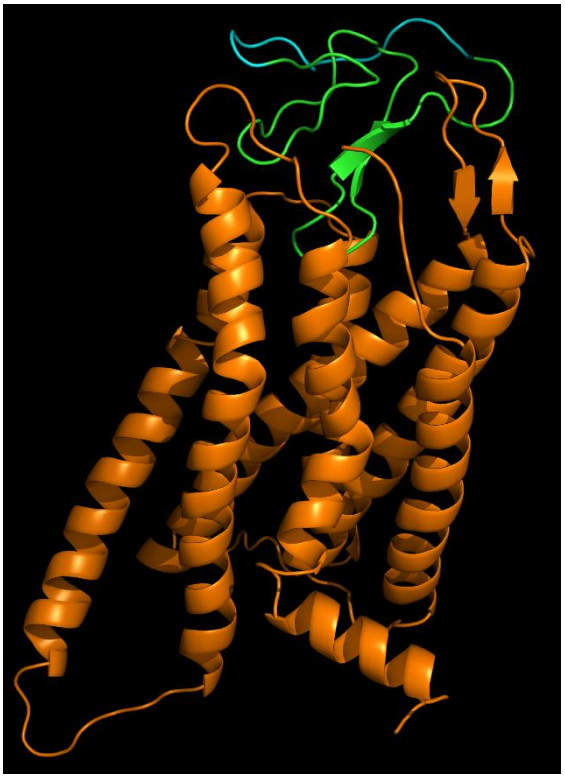

Figure 3.2. Sequence Alterations and Model for Cyclic ASIP
(A) The first line is a portion of the native ASIP sequence with Q115Y/S124Y, known as ASIP-YY. The second sequence shows the new termini for cyclic ASIP after a portion of the sequence (underlined) is shifted to the N-terminus. (B) Model of MC1R (orange) bound to cyclic ASIP (green) with the 13 amino acid linker (cyan) connected to the C-terminus. The linker is distant from the binding pocket of the receptor.

Cyclization Method Selection

There are a variety of published methods for chemical and enzymatic backbone cyclization, and we chose our method based several factors. Firstly, we required a synthetic method compatible with Fmoc solid phase peptide synthesis (SPPS). Our

preliminary studies of these methods also revealed that working with sidechain protected agouti-family peptides in solution was not feasible due to solubility issues. While we had initial cyclization success with traditional native chemical ligation based methods, poor formation of a C-terminal thioester greatly diminished our yields. Recently, Zheng et al. have described a method of peptide cyclization using synthesized peptide hydrazides (31). The peptide hydrazide is easily synthesized using Fmoc SPPS, and is subsequently converted in situ to a thioester to facilitate native chemical ligation with an N-terminal cysteine. We utilized this approach for cyclic ASIP. This approach allowed us to work with side-chain deprotected peptides, greatly increasing our solubility compared to retaining those hydrophobic protecting groups, designed to function in organic solvents.

Resin Preparation and Solid Phase Peptide Synthesis

Cyclic ASIP was synthesized as a peptide hydrazide, necessitating a trityl-$NHNH_2$ resin. We began by converting ChemMatrix trityl-OH resin to trityl-Cl via overnight incubation with a 2% thionyl chloride in DCM. Yields and crude purity of ASIP are greatly enhanced using ChemMatrix resin, which is designed for larger and difficult-to-make peptides. We did attempt to use 2-Cl-(Trt)-Cl resins followed by hydrazination, however we were unable to efficiently couple amino acids to the extent required for ASIP, presumably due to those resins only being available with inadequate, polystyrene supports.

For each synthesis, 240 mg of dry ChemMatrix trityl-OH resin was incubated with 3 mL of 2% $SOCl_2$ in DCM. The following day, trityl-$NHNH_2$ resin was prepared from the trityl-Cl resin using hydrazine hydrate as described in Zheng et al (31). Linear ASIP was synthesized on H-rink amide ChemMatrix resin, giving an amidated C-terminus.

The peptide was synthesized on a Liberty 1 Peptide Synthesizer from CEM Corporation fitted with a Discover Microwave unit using Fmoc chemistry. Fmoc deprotection was achieved with 20% piperidine solution in DMF. All amino acids were double coupled with microwave cycles using 4 equivalents of Fmoc-amino acid in HOBt/DIC, and arginine couplings included an extended coupling. Coupling cycles concluded with a capping step using 10% acetic anhydride in DMF. Linear ASIP was acetylated at the N-terminus by reacting with the same acetic anhydride solution for 5 minutes.

Peptide Cleavage

Fully synthesized peptide resins were split into two reaction vessels, washed with DCM, and dried. For ASIP, in order to prevent aberrant t-butylation of cysteine residues discussed in the previous chapter, linear and cyclic ASIP were cleaved using a modified cocktail consisting of 15 mL TFA, 1 mL TIPS, 2 mL EDT, and 1 mL phenol. The resin was filtered and washed with 10 mL TFA. The combined filtrate and wash was put under a stream of nitrogen gas to evaporate the TFA. After the total volume was reduced to 5 mL, it was then added to 45 mL of cold dry diethyl ether for

precipitation. The precipitate was collected by centrifugation, and the ether was discarded. After a second wash with ether, the pellet was dissolved in 10 mL 2:1 H2O/ACN (0.06% TFA) and lyophilized. Cyclized ASIP had significantly lower crude yields than linear ASIP, despite thorough optimization.

All peptides were purified by reverse phase HPLC on Vydac preparative C18 columns, and fractions collected were analyzed by ESI-MS on a Micromass ZMD mass spectrometer. Peptides corresponding to the correct molecular weight were pooled together and lyophilized. Fractions of ASIP with t-butyl adducts were treated with 300 equivalents of DMSO in TFA with a peptide concentration of 0.2 mg/mL for 1 hour followed by a single ether precipitation. A second wash in ether was unnecessary for this sample and even detrimental because of peptide loss. The pellet was solubilized in 10 mL 2:1 H2O/ACN (0.06% TFA) and lyophilized. The resulting peptide was purified using RP-HPLC and then reduced using 20 mM DTT in 20 mM Tris at pH 7.4 at 37°C for no more than 1 hour. Reduced ASIP will irreversibly precipitate at 37°C after 1 hour.

Native Chemical Ligation

Peptide, purified on a preparative scale, was dissolved in aqueous phosphate buffer (200 mM) at pH 3.0 containing 6 M guanidinium chloride at a concentration of 1 mg/mL peptide. The solution equilibrated for 15 minutes at a temperature of -15°C before the addition of 10 equivalents of $NaNO_2$ from a 0.5 M stock solution. This was also allowed to incubate for 15 minutes at -15°C. It was easier to maintain this low

temperature while using small volumes (<10mL) in a salted ice bath. Concurrently, several small aliquots of peptide in phosphate buffer were equilibrated and incubated with $NaNO_2$. This allowed higher efficiency for the activation step, giving higher overall yields. The aliquots were combined before the room temperature steps described below.

In order to facilitate in situ native chemical ligation, 40 equivalents of 4-mercaptophenylacetic acid (MPAA) was dissolved in phosphate buffer containing 6 M guanidinium chloride at pH 7.0 at a concentration of 10 mg/mL. This was added directly to the peptide solution at room temperature. In order to prevent precipitation, the reaction was diluted to 0.1 mg/mL peptide, using the phosphate buffer. The pH was immediately adjusted to 6.8-7.0. The native chemical ligation reaction was allowed to stir overnight at room temperature before subsequent quenching. Attempting to oxidatively fold ASIP during the cyclization process was impossible due to impurities in the cyclization reaction. Instead, the native chemical ligation solution was reduced with TCEP for 25 minutes and then diluted with 0.06% TFA in water and run on HPLC for purification. Cyclized peptides were confirmed by a mass loss of 32 amu.

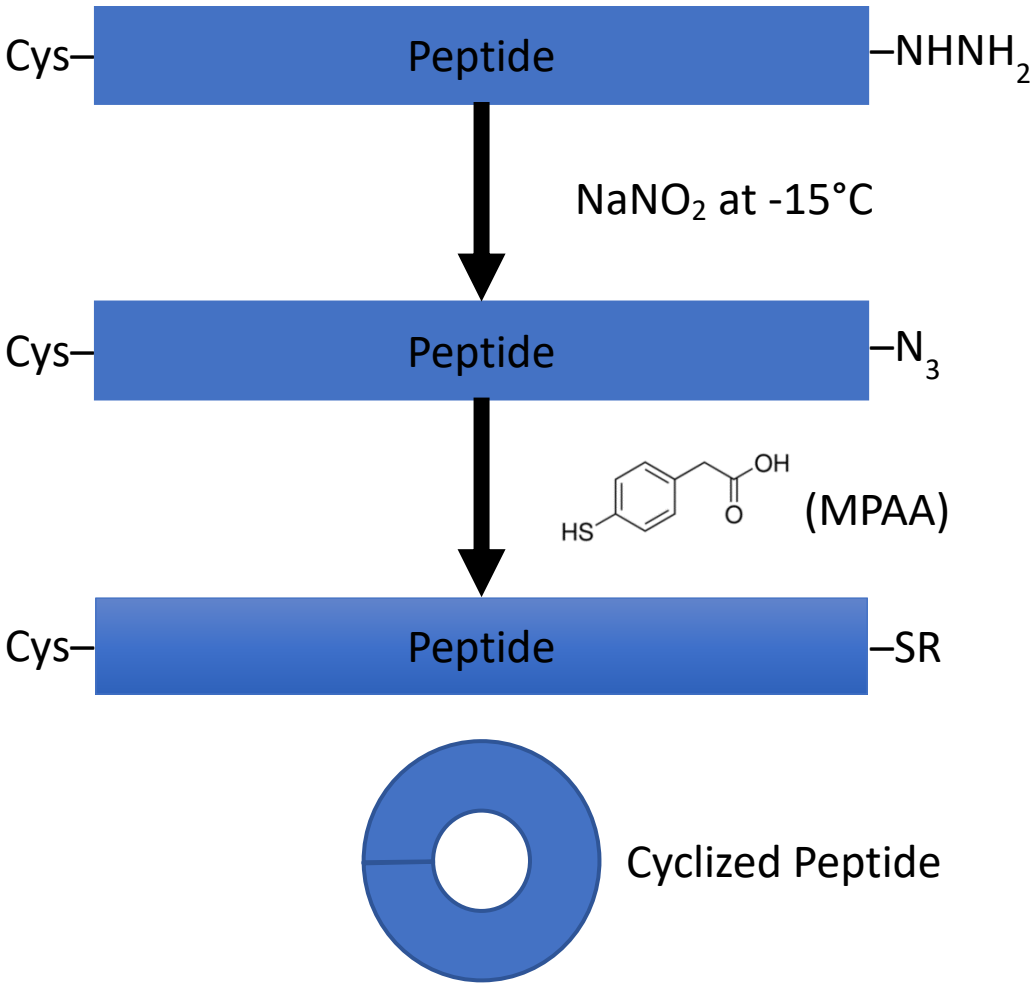

Figure 3.3. Native Chemical Ligation Mechanism
The peptide hydrazide is activated using $NaNO_2$ and then converted to a peptide thioester using MPAA. The thioester interacts with the N-terminal cysteine, bringing the termini in close proximity for subsequent peptide bond formation. This figure was adapted from Zheng et al (31).

Oxidative Folding

Linear and cyclized ASIP were folded according to previously published protocols (30,32). Briefly, ASIP was stirred at room temperature for 27 hours in a buffer consisting of 1.6 M guanidine, 100 mM tris, 5 mM reduced glutathione, 0.5 mM

oxidized glutathione, and 10% DMSO, at pH 7.9. Peptide concentration was typically 0.1 mg/mL.

Folded peptides were purified using RP-HPLC on C18 semi-preparative columns. Via mass spectrometry, we confirmed a mass loss of 10 amu indicating the formation of 5 disulfide bonds. We used NEM to verify that there were no free cysteines. Peptide quantification was done using UV absorption. Folding cyclic ASIP had better yields than its linear counterpart (see Discussion).

Competitive Binding Assay

Ligand binding assays were performed using the DELPHIA europium-based quantification system on human embryonic kidney (HEK) 293T cells transiently transfected with a MC1R construct. This was previously described in Candille et al (33).

cAMP Accumulation Assay

The cAMP experiments were adapted from Patel et al (32). Briefly, cells were incubated in various concentrations of NDP-MSH and 0nM, 10nM or 50nM antagonist. cAMP generation was measured according to the kit protocol. Instead of the HEK 293 cells used by Patel et al., we used melan-A cells.

Nuclear Magnetic Resonance

To confirm cyclic ASIP and linear ASIP had the same fold, homonuclear total correlation spectroscopy (TOCSY) experiments were performed on an 800 MHz

Bruker NMR instrument at room temperature. Both linear and cyclic ASIP were solubilized at a concentration of 400 μM in a buffer consisting of 50 mM d3-acetic acid and 10% D_2O at pH 5.

Serum Stability Assay

Peptides were assessed for their serum stability using a protocol modified from Gunasekera et al (34). 20 μM peptide was incubated at 37°C in human male blood serum (Sigma Aldrich) for up to 24 hours. A negative control was done in phosphate buffered saline (PBS). For both peptides, linear and cyclic, 40 μL aliquots were taken at 0 hours, 1 hour, 3 hours, 5 hours, 8 hours, and 24 hours. These aliquots were quenched by addition of 40 μL of 6 M urea, and then incubated for 10 minutes at 4°C. 40 μL of 6% TFA was then added and again incubated at 4°C. The sample was centrifuged at 13000×g for 10 minutes and loaded on a C18 analytical RP-HPLC column. We used a 1%/min gradient of 5%-50% solvent B (acetonitrile with 0.06% TFA). Elution times of intact peptides were determined by the PBS control at the 0hr time point and verified using mass spectrometry. Percent remaining peptide was determined using integrated 214 nm signal. All experiments were done in triplicate.

Results

Pharmacological Assays

All pharmacology work was done in collaboration with Christopher Kaelin in the Barsh Group. In order to confirm that cyclization had no effect on peptide function, we measured receptor binding by competition binding assays using europium labeled

α-MSH. Linear ASIP and cyclic ASIP both bind tightly to MC1R, with Ki values of 2.4 nM and 2.8 nM respectively (see figure 4.4). They had essentially the same affinity for the receptor.

A

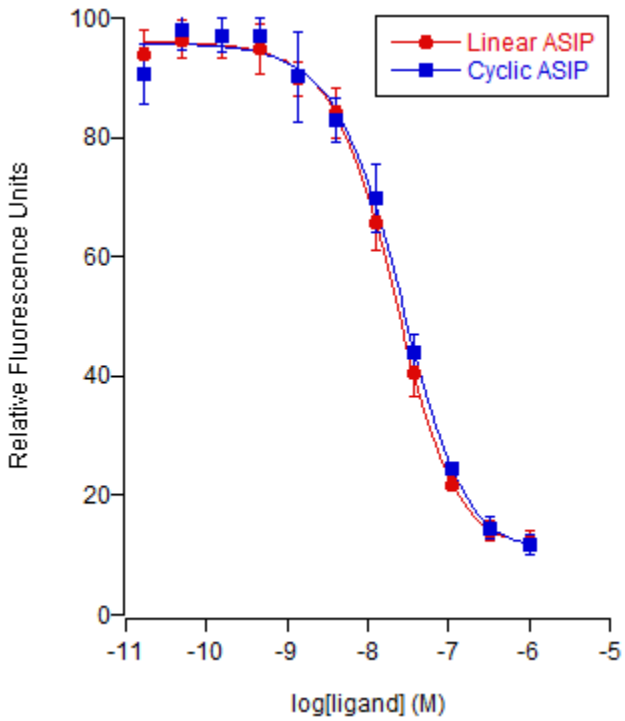

B

Peptide	Ki (nM)	SEM
Linear ASIP	2.398	0.2022
Cyclic ASIP	2.813	0.2145

Figure 3.4. Competitive Binding Assay
(A) Competition binding assay curves comparing linear and cyclic versions of ASIP. The logarithm of antagonist is plotted on the abscissa while the amount of Eu-NDP-MSH bound, measured as relative fluorescence, is plotted on the ordinate. (B) Table of Ki values (in nM) for linear and cyclic ASIP. Mean Ki values (in nM) were calculated by fitting the data to a sigmoidal, dose-response curve with variable slope. All competitive binding experiments were performed in triplicate or greater. Standard error of the mean (SEM) is listed for each peptide.

We also found no difference in inhibition between linear and cyclic ASIP. ASIP normally acts as an antagonist at MC1R, preventing α-MSH from binding and cAMP from accumulating. Patel et al. found that some modifications to ASIP cause loss of inhibition behavior and can even cause ASIP to act as an agonist at MC1R (32). However, this does not occur for cyclic ASIP. We studied the effect of linear and cyclic ASIP, in various concentrations, on the accumulation of cAMP in melan-A cells and found no difference between the two versions of ASIP. This, along with the competition binding assay results, show that backbone cyclization does not lead to a disruption in function of ASIP.

A

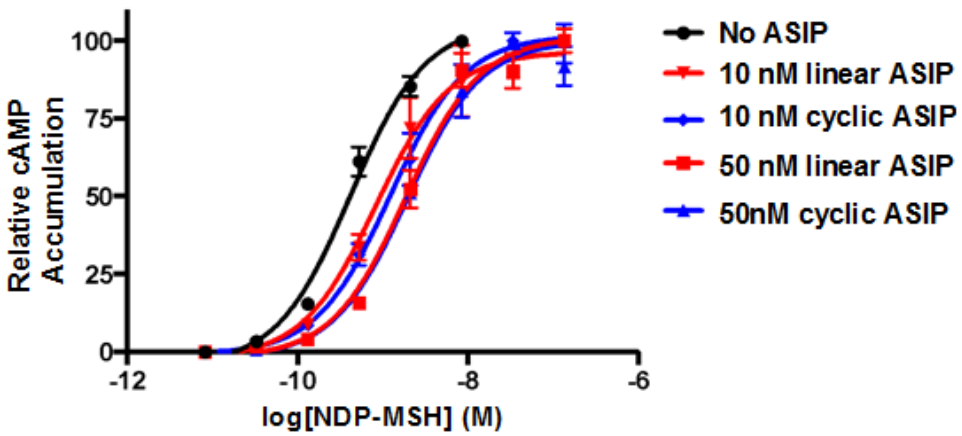

B

Antagonist	Average NDP-MSH EC50 (nM)	SEM
None	0.42	0.05
10 nM linear ASIP	1.04	0.21
10 nM cyclic ASIP	1.48	0.33
50 nM linear ASIP	2.53	0.34
50 nM cyclic ASIP	3.92	1.62

Figure 3.5. cAMP Accumulation Assay

(A) cAMP accumulation assay curves comparing linear and cyclic versions of ASIP. The logarithm of agonist is plotted on the abscissa while the relative amount of cAMP produced is plotted on the ordinate. As more antagonist is added, more NDP-MSH is needed in order to yield the same amount of cAMP. This shifts the curve to the right. Linear and cyclic ASIP have the same antagonistic strength. One replicate is shown in this graph by Christopher Kaelin. (B) Table of half maximal effective concentration (EC50) values (in nM) for NDP-MSH after various concentrations of linear and cyclic ASIP are added. Average EC50 values were calculated by fitting the data to a sigmoidal, dose-response curve with variable slope. All cAMP experiments were performed in triplicate or greater. Standard error of the mean (SEM) is listed for each EC50. This information confirms that there is no statistically significant difference between the effect of linear and cyclic ASIP. For 10 nM and 50 nM concentrations, p= 0.15 and p=0.46 respectively in a paired, two-tailed t-test.

Serum Stability Assay

In order to test whether cyclization increases the proteolytic stability of agouti-family peptides, we compared degradation in human serum between linear and cyclic versions of ASIP over the course of 24 hours. Both versions of the peptide were stable in phosphate buffered saline (PBS) for 24 hours. Linear ASIP showed some proline isomerization in PBS during the time before the samples were run on HPLC. Unexpectedly, cyclic ASIP had much less proline isomerization. It is possible that the reduced flexibility of cyclic ASIP limits the proline conformations. This could increase the activity of cyclic ASIP compared to linear ASIP because the isomerization is more uniform for the cyclic version.

During the initial 5 hours of the assay, linear ASIP showed significantly more degradation than cyclic ASIP in human blood serum. During this initial time, approximately twice as much cyclic ASIP remained, compared to the amount of linear ASIP that was retained. This indicates that cyclizing ASIP confers increased stability and inhibits enzymatic degradation in serum. However, at the 8 hour timepoint, this trend reversed, and slightly less intact cyclic ASIP remained than linear ASIP. The decrease in proteolysis of linear ASIP in the later time points is likely due to product inhibition. After 24 hours, cyclic ASIP cannot be observed via UV absorption or mass spectrometry. Approximately 5% of the original linear ASIP remained. Both versions of ASIP had less than 10% peptide remaining at 24 hours.

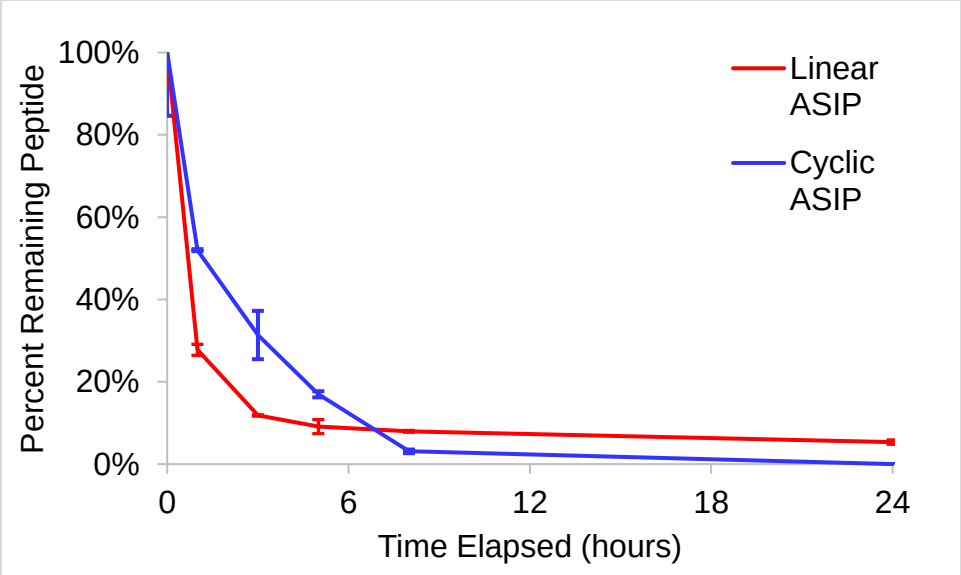

Figure 3.6. Serum Stability Assay
Percentage of peptide remaining after 24 hours in human blood serum. All timepoints were done in triplicate.

NMR Results

Introduction of a head-to-tail peptide bond may impose a constraint that distorts the native structure. We used nuclear magnetic resonance spectroscopy (NMR) to confirm that the knottin structures were not perturbed. We completed homonuclear TOCSY NMR for ASIP to observe if the resultant cyclic spectra overlaid with that of linear ASIP. Many peaks for linear and cyclic ASIP within the fingerprint region of the spectra aligned closely or with only slight shifts (Figure 4.7), suggesting that the two peptides adopt similar folds. Inspection of the NMR spectra confirms that the beta sheet possessed by linear ASIP is retained by cyclic ASIP. The peaks in the fingerprint region are similarly dispersed, indicating that the two peptides have

similar packing and hydrophobic surface characteristics. Differences in the spectra are expected, due to new peaks arising from the newly restrained linker region, as well as new interactions between the N-terminus and the structured domain. The data demonstrate that ligation of the random coil 13 amino acid N-terminus to the C-terminus did not perturb the peptide's ability to fold properly.

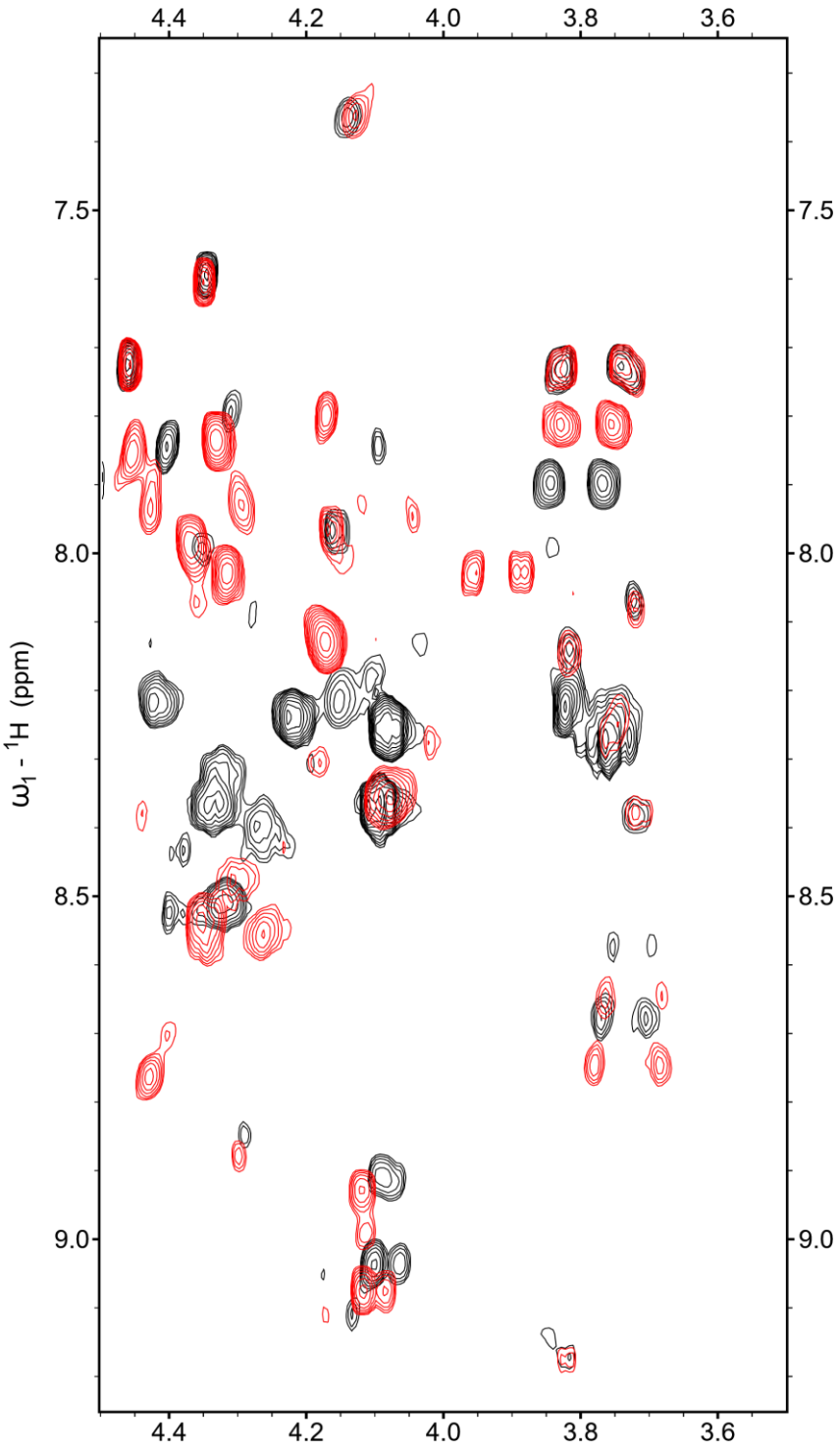

Figure 3.7. Selected Region of the TOCSY Spectra for Linear and Cyclic ASIP

The black spectrum is from linear ASIP. The red spectrum is from cyclic ASIP and shows overlapping peaks, some chemical shift changes, and some new peaks from the linker region.

Discussion

We have successfully produced head-to-tail cyclized versions of agouti-family knottin peptides using native chemical ligation via peptide hydrazide intermediates. This method, once optimized, robustly produced cyclized versions of large, difficult-to-make peptides in a manner compatible with standard Fmoc chemistry. This relatively new approach to the synthesis of cyclic peptides has been reported elsewhere to be an efficient approach, and our results largely agree. As expected, ASIP did not require an additional linker region for proper ligation and folding.

Interestingly, folding of cyclic ASIP resulted in significantly higher yields, compared to oxidative folding of ASIP with free termini. Disulfide bond formation of ASIP usually results in peptide loss due to the formation of glutathione adducts and misfolded protein. After cyclization, substantially more protein was found in the major folded peak, and less glutathione adducts formed. This benefit to peptide folding parallels with work done by Daly et al (19). We hypothesized that the lack of conformational freedom in cyclic ASIP causes entropic benefits to the folding process.

Our data demonstrate the cyclization of agouti-family knottins does not perturb their structure or function. NMR data confirmed that the structure of the cyclic peptides matched that of uncyclized. We tested biological activity of cyclic ASIP by its ability to bind MC1R, its natural biological target. The wild-type ASIP exhibits high-affinity binding at this receptor as an endogenous antagonist to the agonist α-MSH. Cyclic

ASIP retained this high-affinity binding to MC1R. However, we did not find any enhancement of affinity to the receptor as others have observed as a benefit of cyclization (20,21).

We had hypothesized that peptide cyclization would increase resistance to proteolysis cleavage, potentially by reduced susceptibility to exoproteases due to removal of free termini, and increased peptide rigidity, hampering endoproteases. Cyclic ASIP exhibited increased stability during the initial five hours of the human serum stability assays we employed, though this protection was diminished by 24 hours. These results are consistent with the varying degrees of success of knottin cyclization compared to non-knottin, disulfide-rich peptides. Cyclized knottins have shown smaller increases compared to small, non-ICK peptides in terms of their serum stability. This indicates that the agouti-family peptides, and knottins in general, already possess exquisite stability, though cyclized ASIP's small increase in stability may have relevance for use as a therapeutic.

In separate LC-MS experiments, we measured the molecular weights and prevalence of the degraded peptide fragments from the serum stability assay. Between 3 hours and 8 hours in serum, cyclic ASIP that has undergone a single hydrolysis event (+18 Da) is by far the most abundant species of ASIP. After cyclic ASIP is hydrolyzed in one location, it is no longer has the stability benefits displayed by cyclic peptides. However, depending on where it is hydrolyzed, cyclic ASIP could be functional at the receptor. After all, ASIP-YY is a form of "cut" cyclic ASIP and is conclusively

functional. Studies in vivo might show a remarkable increase in longevity of the therapeutic that is not seen in the serum assay.

There are several interesting implications of our results. Pretreatment of melanoma cells with ASIP has been shown to increase the effectiveness of traditional chemotherapeutics 2- to 3-fold (29). This means ASIP could reduce the amount of toxic chemotherapy treatments necessary. Increasing the stability of this peptide at any level could prove to have a significant effect on its ability to manage melanoma. Cyclic ASIP was more stable than linear ASIP throughout the first 5 hours. During this period, cyclic ASIP could sufficiently reduce melanosome production and cause increased chemotherapy efficacy before it is degraded in the body.

More generally, our results demonstrate the feasibility of peptide head-to-tail cyclization to the agouti-family of knottin peptides. Disulfide-rich peptides are currently showing promise as scaffolds for drug design and imaging purposes. Along with the potential for improved biological stability, cyclization adds a functional loop that is amendable to amino acid substitution for the purposes of drug design. We hope that the expanded applicability of peptide cyclization will motivate future efforts in knottin drug design and stabilization.

References

1. Craik DJ, Fairlie DP, Liras S, Price D. The Future of Peptide-based Drugs. Chem Biol Drug Des. 2013 Jan 1;81(1):136–47.

2. Fosgerau K, Hoffmann T. Peptide therapeutics: current status and future directions. Drug Discov Today. 2015 Jan;20(1):122–8.

3. Dharanipragada R. New modalities in conformationally constrained peptides for potency, selectivity and cell permeation. Future Med Chem. 2013 May 1;5(7):831–49.

4. Piekielna J, Perlikowska R, Gach K, Janecka A. Cyclization in Opioid Peptides. Curr Drug Targets. 2013 Jun 1;14(7):798–816.

5. Daly NL, Craik DJ. Bioactive cystine knot proteins. Curr Opin Chem Biol. 2011 Jun;15(3):362–8.

6. Kintzing JR, Cochran JR. Engineered knottin peptides as diagnostics, therapeutics, and drug delivery vehicles. Curr Opin Chem Biol. 2016 Oct;34:143–50.

7. Moore SJ, Leung CL, Cochran JR. Knottins: disulfide-bonded therapeutic and diagnostic peptides. Drug Discov Today Technol. 2012;9(1):e3–11.

8. Kolmar H. Alternative binding proteins: Biological activity and therapeutic potential of cystine-knot miniproteins. FEBS J. 2008 Jun 1;275(11):2684–90.

9. Kolmar H. Biological diversity and therapeutic potential of natural and engineered cystine knot miniproteins. Curr Opin Pharmacol. 2009 Oct;9(5):608–14.

10. Li H, Su M, Hamann MT, Bowling JJ, Kim HS, Jung JH. Solution Structure of a Sponge-Derived Cystine Knot Peptide and Its Notable Stability. J Nat Prod [Internet]. 2014 Feb 5 [cited 2014 Feb 13]; Available from: http://dx.doi.org/10.1021/np400899a

11. Craik DJ, Daly NL, Waine C. The cystine knot motif in toxins and implications for drug design. Toxicon Off J Int Soc Toxinology. 2001 Jan;39(1):43–60.

12. Burman R, Gunasekera S, Strömstedt AA, Göransson U. Chemistry and Biology of Cyclotides: Circular Plant Peptides Outside the Box. J Nat Prod [Internet]. 2014 Feb 14 [cited 2014 Feb 18]; Available from: http://dx.doi.org/10.1021/np401055j

13. Craik DJ. Circling the enemy: cyclic proteins in plant defence. Trends Plant Sci. 2009 Jun;14(6):328–35.

14. Ji Y, Majumder S, Millard M, Borra R, Bi T, Elnagar AY, et al. In Vivo Activation of the p53 Tumor Suppressor Pathway by an Engineered Cyclotide. J Am Chem Soc. 2013 Aug 7;135(31):11623–33.

15. Weidmann J, Craik DJ. Discovery, structure, function, and applications of cyclotides: circular proteins from plants. J Exp Bot. 2016 Aug 1;67(16):4801–12.

16. Clark RJ, Fischer H, Dempster L, Daly NL, Rosengren KJ, Nevin ST, et al. Engineering stable peptide toxins by means of backbone cyclization: Stabilization of the α-conotoxin MII. Proc Natl Acad Sci U S A. 2005 Sep 27;102(39):13767–72.

17. Clark RJ, Jensen J, Nevin ST, Callaghan BP, Adams DJ, Craik DJ. The Engineering of an Orally Active Conotoxin for the Treatment of Neuropathic Pain. Angew Chem Int Ed. 2010 Sep 3;49(37):6545–8.

18. Wang CK, Swedberg JE, Northfield SE, Craik DJ. Effects of Cyclization on Peptide Backbone Dynamics. J Phys Chem B. 2015 Dec 31;119(52):15821–30.

19. Daly NL, Love S, Alewood PF, Craik DJ. Chemical Synthesis and Folding Pathways of Large Cyclic Polypeptides: Studies of the Cystine Knot Polypeptide Kalata B1†. Biochemistry (Mosc). 1999 Aug 1;38(32):10606–14.

20. Akcan M, Clark RJ, Daly NL, Conibear AC, de Faoite A, Heghinian MD, et al. Transforming conotoxins into cyclotides: Backbone cyclization of P-superfamily conotoxins. Pept Sci. 2015 Nov 1;104(6):682–92.

21. Heitz A, Avrutina O, Le-Nguyen D, Diederichsen U, Hernandez J-F, Gracy J, et al. Knottin cyclization: impact on structure and dynamics. BMC Struct Biol. 2008 Dec 12;8(1):54.

22. Kwon S, Bosmans F, Kaas Q, Cheneval O, Conibear AC, Rosengren KJ, et al. Efficient enzymatic cyclization of an inhibitory cystine knot-containing peptide. Biotechnol Bioeng. 2016 Oct 1;113(10):2202–12.

23. Cooray SN, Clark AJL. Melanocortin receptors and their accessory proteins. Mol Cell Endocrinol. 2011 Jan 15;331(2):215–21.

24. Bultman SJ, Michaud EJ, Woychik RP. Molecular characterization of the mouse agouti locus. Cell. 1992 Dec 24;71(7):1195–204.

25. Farooqi IS, O'Rahilly S. Mutations in ligands and receptors of the leptin–melanocortin pathway that lead to obesity. Nat Rev Endocrinol. 2008 Sep 9;4(10):569–77.

26. Hagan MM, Benoit SC, Rushing PA, Pritchard LM, Woods SC, Seeley RJ. Immediate and Prolonged Patterns of Agouti-Related Peptide-(83–132)-Induced c-

Fos Activation in Hypothalamic and Extrahypothalamic Sites. Endocrinology. 2001 Mar 1;142(3):1050–6.

27. Hoggard N, Johnstone AM, Faber P, Gibney ER, Elia M, Lobley G, et al. Plasma concentrations of α-MSH, AgRP and leptin in lean and obese men and their relationship to differing states of energy balance perturbation. Clin Endocrinol (Oxf). 2004;61(1):31–39.

28. Shen C-P, Wu KK, Shearman LP, Camacho R, Tota MR, Fong TM, et al. Plasma Agouti-Related Protein Level: A Possible Correlation with Fasted and Fed States in Humans and Rats. J Neuroendocrinol. 2002;14(8):607–610.

29. Huang Z, Chinen M, Chang PJ, Xie T, Zhong L, Demetriou S, et al. Targeting protein-trafficking pathways alters melanoma treatment sensitivity. Proc Natl Acad Sci U S A. 2012 Jan 10;109(2):553–8.

30. McNulty JC, Jackson PJ, Thompson DA, Chai B, Gantz I, Barsh GS, et al. Structures of the Agouti Signaling Protein. J Mol Biol. 2005 Mar 4;346(4):1059–70.

31. Zheng J-S, Tang S, Qi Y-K, Wang Z-P, Liu L. Chemical synthesis of proteins using peptide hydrazides as thioester surrogates. Nat Protoc. 2013 Dec;8(12):2483–95.

32. Patel MP, Cribb Fabersunne CS, Yang Y, Kaelin CB, Barsh GS, Millhauser GL. Loop-Swapped Chimeras of the Agouti-Related Protein and the Agouti Signaling Protein Identify Contacts Required for Melanocortin 1 Receptor Selectivity and Antagonism. J Mol Biol. 2010 Nov 19;404(1):45–55.

33. Candille SI, Kaelin CB, Cattanach BM, Yu B, Thompson DA, Nix MA, et al. A B-defensin mutation causes black coat color in domestic dogs. Science. 2007 Nov 30;318(5855):1418–23.

34. Gunasekera S, Foley FM, Clark RJ, Sando L, Fabri LJ, Craik DJ, et al. Engineering Stabilized Vascular Endothelial Growth Factor-A Antagonists: Synthesis, Structural Characterization, and Bioactivity of Grafted Analogues of Cyclotides. J Med Chem. 2008 Dec 25;51(24):7697–704.

BIBLIOGRAPHY

2iqr » Melanocortin-4 receptor model (active state) with agonist NDP-MSH - Orientations of Proteins in Membranes (OPM) database [Internet]. [cited 2016 Dec 3]. Available from: http://opm.phar.umich.edu/protein.php?pdbid=2iqr

Abdel-Malek ZA, Knittel J, Kadekaro AL, Swope VB, Starner R. The melanocortin 1 receptor and the UV response of human melanocytes--a shift in paradigm. Photochem Photobiol. 2008 Apr;84(2):501–8.

Abdel-Malek ZA. Melanocortin receptors: their functions and regulation by physiological agonists and antagonists. Cell Mol Life Sci CMLS. 2001 Mar;58(3):434–41.

Akcan M, Clark RJ, Daly NL, Conibear AC, de Faoite A, Heghinian MD, et al. Transforming conotoxins into cyclotides: Backbone cyclization of P-superfamily conotoxins. Pept Sci. 2015 Nov 1;104(6):682–92.

Barsh G, Gunn T, He L, Schlossman S, Duke-Cohan J. Biochemical and genetic studies of pigment-type switching. Pigment Cell Res. 2000;13 Suppl 8:48–53.

Bednarek MA, Silva MV, Arison B, MacNeil T, Kalyani RN, Huang RR, et al. Structure-function studies on the cyclic peptide MT-II, lactam derivative of alpha-melanotropin. Peptides. 1999;20(3):401–9.

Bultman SJ, Michaud EJ, Woychik RP. Molecular characterization of the mouse agouti locus. Cell. 1992 Dec 24;71(7):1195–204.

Burman R, Gunasekera S, Strömstedt AA, Göransson U. Chemistry and Biology of Cyclotides: Circular Plant Peptides Outside the Box. J Nat Prod [Internet]. 2014 Feb 14 [cited 2014 Feb 18]; Available from: http://dx.doi.org/10.1021/np401055j

Candille SI, Kaelin CB, Cattanach BM, Yu B, Thompson DA, Nix MA, et al. A B-defensin mutation causes black coat color in domestic dogs. Science. 2007 Nov 30;318(5855):1418–23.

Chai B-X, Pogozheva ID, Lai Y-M, Li J-Y, Neubig RR, Mosberg HI, et al. Receptor−Antagonist Interactions in the Complexes of Agouti and Agouti-Related Protein with Human Melanocortin 1 and 4 Receptors † , ‡. Biochemistry (Mosc). 2005 Mar;44(9):3418–31.

Chen KG, Leapman RD, Zhang G, Lai B, Valencia JC, Cardarelli CO, et al. Influence of melanosome dynamics on melanoma drug sensitivity. J Natl Cancer Inst. 2009 Sep 16;101(18):1259–71.

Clark RJ, Fischer H, Dempster L, Daly NL, Rosengren KJ, Nevin ST, et al. Engineering stable peptide toxins by means of backbone cyclization: Stabilization of the α-conotoxin MII. Proc Natl Acad Sci U S A. 2005 Sep 27;102(39):13767–72.

Clark RJ, Jensen J, Nevin ST, Callaghan BP, Adams DJ, Craik DJ. The Engineering of an Orally Active Conotoxin for the Treatment of Neuropathic Pain. Angew Chem Int Ed. 2010 Sep 3;49(37):6545–8.

Cooray SN, Clark AJL. Melanocortin receptors and their accessory proteins. Mol Cell Endocrinol. 2011 Jan 15;331(2):215–21.

Craik DJ, Daly NL, Waine C. The cystine knot motif in toxins and implications for drug design. Toxicon Off J Int Soc Toxinology. 2001 Jan;39(1):43–60.

Craik DJ, Fairlie DP, Liras S, Price D. The Future of Peptide-based Drugs. Chem Biol Drug Des. 2013 Jan 1;81(1):136–47.

Craik DJ. Circling the enemy: cyclic proteins in plant defence. Trends Plant Sci. 2009 Jun;14(6):328–35.

Daly NL, Craik DJ. Bioactive cystine knot proteins. Curr Opin Chem Biol. 2011 Jun;15(3):362–8.

Daly NL, Love S, Alewood PF, Craik DJ. Chemical Synthesis and Folding Pathways of Large Cyclic Polypeptides: Studies of the Cystine Knot Polypeptide Kalata B1†. Biochemistry (Mosc). 1999 Aug 1;38(32):10606–14.

Dharanipragada R. New modalities in conformationally constrained peptides for potency, selectivity and cell permeation. Future Med Chem. 2013 May 1;5(7):831–49.

Ersoy BA, Pardo L, Zhang S, Thompson DA, Millhauser G, Govaerts C, et al. Mechanism of N-terminal modulation of activity at the melanocortin-4 receptor GPCR. Nat Chem Biol. 2012 Jun 24;8(8):725–30.

Farooqi IS, O'Rahilly S. Mutations in ligands and receptors of the leptin–melanocortin pathway that lead to obesity. Nat Rev Endocrinol. 2008 Sep 9;4(10):569–77.

Fosgerau K, Hoffmann T. Peptide therapeutics: current status and future directions. Drug Discov Today. 2015 Jan;20(1):122–8.

Fredriksson R, Lagerström MC, Lundin L-G, Schiöth HB. The G-protein-coupled receptors in the human genome form five main families. Phylogenetic

analysis, paralogon groups, and fingerprints. Mol Pharmacol. 2003 Jun;63(6):1256–72.

Gantz I, Fong TM. The melanocortin system. Am J Physiol Endocrinol Metab. 2003 Mar;284(3):E468-474.

Gilman AG. G proteins: transducers of receptor-generated signals. Annu Rev Biochem. 1987;56:615–49.

Gunasekera S, Foley FM, Clark RJ, Sando L, Fabri LJ, Craik DJ, et al. Engineering Stabilized Vascular Endothelial Growth Factor-A Antagonists: Synthesis, Structural Characterization, and Bioactivity of Grafted Analogues of Cyclotides. J Med Chem. 2008 Dec 25;51(24):7697–704.

Hadley ME, Haskell-Luevano C. The proopiomelanocortin system. Ann N Y Acad Sci. 1999 Oct 20;885:1–21.

Hagan MM, Benoit SC, Rushing PA, Pritchard LM, Woods SC, Seeley RJ. Immediate and Prolonged Patterns of Agouti-Related Peptide-(83–132)-Induced c-Fos Activation in Hypothalamic and Extrahypothalamic Sites. Endocrinology. 2001 Mar 1;142(3):1050–6.

Hanson MA, Stevens RC. Discovery of new GPCR biology: one receptor structure at a time. Struct Lond Engl 1993. 2009 Jan 14;17(1):8–14.

Heitz A, Avrutina O, Le-Nguyen D, Diederichsen U, Hernandez J-F, Gracy J, et al. Knottin cyclization: impact on structure and dynamics. BMC Struct Biol. 2008 Dec 12;8(1):54.

Hoggard N, Johnstone AM, Faber P, Gibney ER, Elia M, Lobley G, et al. Plasma concentrations of α-MSH, AgRP and leptin in lean and obese men and their relationship to differing states of energy balance perturbation. Clin Endocrinol (Oxf). 2004;61(1):31–39.

Huang Z -m., Chinen M, Chang PJ, Xie T, Zhong L, Demetriou S, et al. Targeting protein-trafficking pathways alters melanoma treatment sensitivity. Proc Natl Acad Sci. 2012 Jan 10;109(2):553–8.

Jackson PJ, McNulty JC, Yang Y-K, Thompson DA, Chai B, Gantz I, et al. Design, pharmacology, and NMR structure of a minimized cystine knot with agouti-related protein activity. Biochemistry (Mosc). 2002 Jun 18;41(24):7565–72.

Ji Y, Majumder S, Millard M, Borra R, Bi T, Elnagar AY, et al. In Vivo Activation of the p53 Tumor Suppressor Pathway by an Engineered Cyclotide. J Am Chem Soc. 2013 Aug 7;135(31):11623–33.

Key statistics for melanoma skin cancer [Internet]. [cited 2016 Dec 1]. Available from: http://www.cancer.org/cancer/skincancer-melanoma/detailedguide/melanoma-skin-cancer-key-statistics

Kiefer LL, Veal JM, Mountjoy KG, Wilkison WO. Melanocortin receptor binding determinants in the agouti protein. Biochemistry (Mosc). 1998 Jan 27;37(4):991–7.

Kintzing JR, Cochran JR. Engineered knottin peptides as diagnostics, therapeutics, and drug delivery vehicles. Curr Opin Chem Biol. 2016 Oct;34:143–50.

Kolmar H. Alternative binding proteins: Biological activity and therapeutic potential of cystine-knot miniproteins. FEBS J. 2008 Jun 1;275(11):2684–90.

Kolmar H. Biological diversity and therapeutic potential of natural and engineered cystine knot miniproteins. Curr Opin Pharmacol. 2009 Oct;9(5):608–14.

Kwon S, Bosmans F, Kaas Q, Cheneval O, Conibear AC, Rosengren KJ, et al. Efficient enzymatic cyclization of an inhibitory cystine knot-containing peptide. Biotechnol Bioeng. 2016 Oct 1;113(10):2202–12.

Li H, Su M, Hamann MT, Bowling JJ, Kim HS, Jung JH. Solution Structure of a Sponge-Derived Cystine Knot Peptide and Its Notable Stability. J Nat Prod [Internet]. 2014 Feb 5 [cited 2014 Feb 13]; Available from: http://dx.doi.org/10.1021/np400899a

Lukszo J, Patterson D, Albericio F, Kates SA. 3-(1-Piperidinyl)alanine formation during the preparation ofC-terminal cysteine peptides with the Fmoc/t-Bu strategy. Lett Pept Sci. 1996 Jul;3(3):157–66.

Madonna ME, Schurdak J, Yang Y-K, Benoit S, Millhauser GL. Agouti-related protein segments outside of the receptor binding core are required for enhanced short- and long-term feeding stimulation. ACS Chem Biol. 2012 Feb 17;7(2):395–402.

McNulty JC, Jackson PJ, Thompson DA, Chai B, Gantz I, Barsh GS, et al. Structures of the agouti signaling protein. J Mol Biol. 2005 Mar 4;346(4):1059–70.

McNulty JC, Thompson DA, Bolin KA, Wilken J, Barsh GS, Millhauser GL. High-resolution NMR structure of the chemically-synthesized melanocortin receptor binding domain AGRP(87-132) of the agouti-related protein. Biochemistry (Mosc). 2001 Dec 25;40(51):15520–7.

Milligan G. Constitutive activity and inverse agonists of G protein-coupled receptors: a current perspective. Mol Pharmacol. 2003 Dec;64(6):1271–6.

Moore SJ, Leung CL, Cochran JR. Knottins: disulfide-bonded therapeutic and diagnostic peptides. Drug Discov Today Technol. 2012;9(1):e3–11.

Mountjoy KG. The human melanocyte stimulating hormone receptor has evolved to become “super-sensitive” to melanocortin peptides. Mol Cell Endocrinol. 1994 Jun;102(1–2):R7-11.

Nix MA, Kaelin CB, Palomino R, Miller JL, Barsh GS, Millhauser GL. Electrostatic Similarity Analysis of Human β-Defensin Binding in the Melanocortin System. Biophys J. 2015 Nov;109(9):1946–58.

Nix MA, Kaelin CB, Ta T, Weis A, Morton GJ, Barsh GS, et al. Molecular and Functional Analysis of Human β-Defensin 3 Action at Melanocortin Receptors. Chem Biol. 2013 Jun;20(6):784–95.

Ollmann MM, Wilson BD, Yang YK, Kerns JA, Chen Y, Gantz I, et al. Antagonism of central melanocortin receptors in vitro and in vivo by agouti-related protein. Science. 1997 Oct 3;278(5335):135–8.

Patel MP, Cribb Fabersunne CS, Yang Y, Kaelin CB, Barsh GS, Millhauser GL. Loop-Swapped Chimeras of the Agouti-Related Protein and the Agouti Signaling Protein Identify Contacts Required for Melanocortin 1 Receptor Selectivity and Antagonism. J Mol Biol. 2010 Nov;404(1):45–55.

Pazgier M, Hoover DM, Yang D, Lu W, Lubkowski J. Human β-defensins. Cell Mol Life Sci CMLS. 2006 Jun 1;63(11):1294–313.

Piekielna J, Perlikowska R, Gach K, Janecka A. Cyclization in Opioid Peptides. Curr Drug Targets. 2013 Jun 1;14(7):798–816.

Pogozheva ID, Chai B-X, Lomize AL, Fong TM, Weinberg DH, Nargund RP, et al. Interactions of human melanocortin 4 receptor with nonpeptide and peptide agonists. Biochemistry (Mosc). 2005 Aug 30;44(34):11329–41.

Reizes O, Clegg DJ, Strader AD, Benoit SC. A role for syndecan-3 in the melanocortin regulation of energy balance. Peptides. 2006 Feb;27(2):274–80.

Shen C-P, Wu KK, Shearman LP, Camacho R, Tota MR, Fong TM, et al. Plasma Agouti-Related Protein Level: A Possible Correlation with Fasted and Fed States in Humans and Rats. J Neuroendocrinol. 2002;14(8):607–610.

Skin Cancer - Melanoma | American Cancer Society [Internet]. [cited 2016 Dec 1]. Available from: http://www.cancer.org/cancer/skincancer-melanoma/

Wang CK, Swedberg JE, Northfield SE, Craik DJ. Effects of Cyclization on Peptide Backbone Dynamics. J Phys Chem B. 2015 Dec 31;119(52):15821–30.

Weidmann J, Craik DJ. Discovery, structure, function, and applications of cyclotides: circular proteins from plants. J Exp Bot. 2016 Aug 1;67(16):4801–12.

Wikberg JE, Muceniece R, Mandrika I, Prusis P, Lindblom J, Post C, et al. New aspects on the melanocortins and their receptors. Pharmacol Res. 2000 Nov;42(5):393–420.

Wikberg JE. Melanocortin receptors: perspectives for novel drugs. Eur J Pharmacol. 1999 Jun 30;375(1–3):295–310.

Wintzen M, Gilchrest BA. Proopiomelanocortin, its derived peptides, and the skin. J Invest Dermatol. 1996 Jan;106(1):3–10.

Wu X, Wu Y, Zhu F, Yang Q, Wu Q, Zhangsun D, et al. Optimal Cleavage and Oxidative Folding of α-Conotoxin TxIB as a Therapeutic Candidate Peptide. Mar Drugs. 2013 Sep 17;11(9):3537–53.

Yang D, Chertov O, Bykovskaia SN, Chen Q, Buffo MJ, Shogan J, et al. Beta-defensins: linking innate and adaptive immunity through dendritic and T cell CCR6. Science. 1999 Oct 15;286(5439):525–8.

Zheng J-S, Tang S, Qi Y-K, Wang Z-P, Liu L. Chemical synthesis of proteins using peptide hydrazides as thioester surrogates. Nat Protoc. 2013 Dec;8(12):2483–95.